Fractal Growth Phenomena

Tamás Vicsek

Institute for Technical Physics
Budapest, Hungary

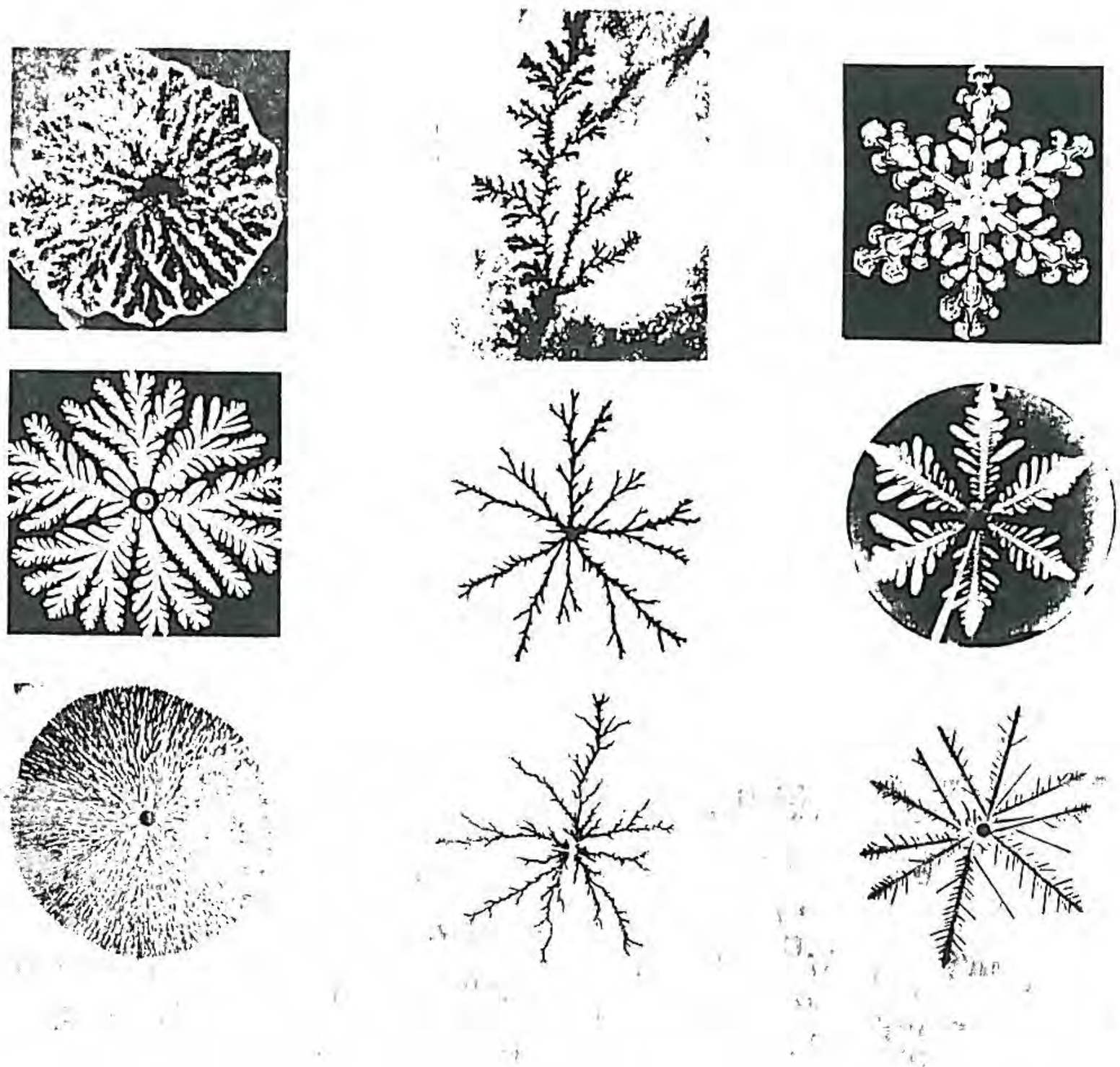

WORLD SCIENTIFIC
Singapore

$D = A \cdot b^{\alpha}$

/

Scaling, $C(r) \sim A r^{\alpha}$ $r \to br$ $C(br) \sim D r^{\alpha}$
new - analitikus, kritikus viselkedés, kritikus pont
universális kritikus exponenser

PART II.

CLUSTER GROWTH MODELS

Chapter 8.

CLUSTER-CLUSTER AGGREGATION

Aggregation of microscopic particles diffusing in a fluid medium represents a common process leading to fractal structures. If the density of the initially randomly distributed particles is larger than zero, the probability for two "sticky" particles to collide and stick together is finite. It is typical for such systems that the resulting two-particle aggregate can diffuse further and may form larger fractal clusters by joining other aggregates (Friedlander 1977). As a result the mean cluster size increases in time and, in principle, after a sufficiently long period all of the particles in the finite system become part of a single cluster. In many cases the force between two particles is of short range and it is strong enough to bind the particles irreversibly when they contact each other. For example, such behaviour can be observed for iron smoke aggregates formed in air (Forrest and Witten 1979) or in aqueous gold colloids (Weitz and Olivera 1984).

In the above process each cluster is equivalent with regard to the conditions for their motion, i.e., there is no seed particle as in the case of DLA. Consequently, this process is called cluster-cluster aggregation (CCA) to distinguish it from particle-cluster aggregation phenomena discussed in the previous sections of Part II. CCA directly corresponds to the physical situation taking place in a system of aggregating particles, in contrast to DLA which in general should be regarded as a computer model for phenomena not

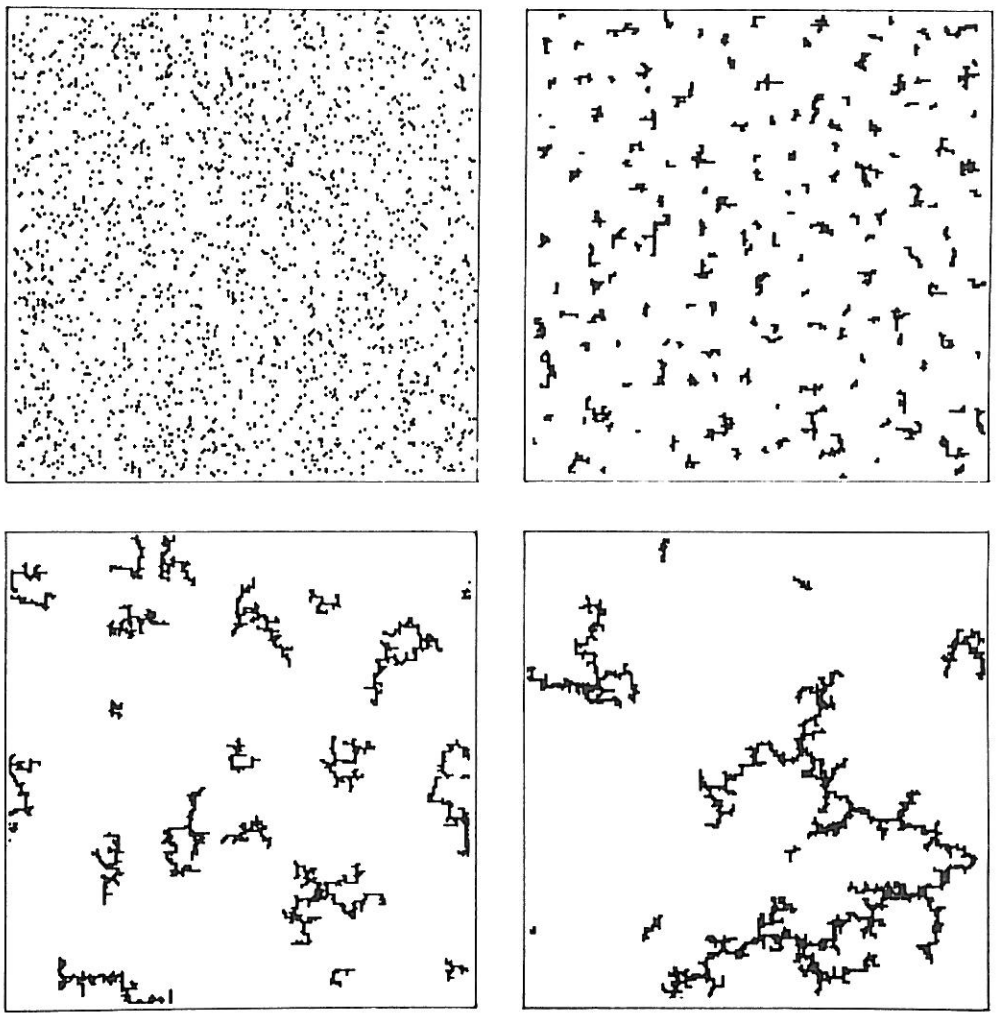

Figure 8.1. Snapshots of configurations taken at various "times" during the computer simulation of diffusion-limited cluster-cluster aggregation in two dimensions.

necessarily involving attachment of particles.

The possibility of simulating colloidal aggregation in a computer has been recognized for a few decades (Sutherland 1967). However, large scale numerical investigation of cluster-cluster aggregation has become feasible only in recent years. Simple *computer models* for CCA (e.g. Meakin 1983c, Kolb *et al* 1983) can be successfully used to study the structure of aggregates and the dynamics of their formation. A typical two-dimensional simulation is started by randomly occupying a small fraction of the sites on a square lattice to represent particles. At each time step a particle or a cluster is

selected randomly and is moved by one lattice unit in a randomly chosen direction. Two clusters stick when they touch each other. Fig. 8.1 shows four stages of such a process. This figure demonstrates the most important properties of cluster-cluster aggregation. With increasing time the number of clusters decreases, and large, randomly branching aggregates appear in the system. The computer generated clusters and the real aggregates observed in many recent experiments were found to have very similar fractal scaling.

Because of the simultaneous diffusional motion of aggregates, the time is a well defined quantity in CCA (including simulations). Accordingly, the related numerical and experimental investigations have concentrated on both the *geometrical and dynamical* aspects of the aggregation process. The results suggest that in analogy with equilibrium phase transitions, non-trivial scaling can be found in both approaches. Therefore, in addition to the fractal structure of aggregates, in this Chapter we shall discuss the dynamic scaling for the cluster size distribution as well (Vicsek and Family 1984, Kolb 1984).

Most of the real cluster-cluster aggregation processes are more complex than the simple simulation described above. It is mainly the shape of the short-range interaction potential between two particles which determines the nature of the statics and dynamics of CCA. A deep minimum in the potential and a negligible repulsion part results in the so-called i) *diffusion-limited* regime, when two clusters stick rigidly together as soon as they contact. The relevant time scale in this process is the typical time needed for two diffusing clusters to approach each other. During ii) *reaction-limited* (or chemically-limited) CCA a small, but relevant repulsive potential barrier can prevent the clusters from joining each other even if they are close. However, after a number of contacts they may become joined irreversibly. In this case it is the time needed for the formation of a bond between adjacent clusters which determines the characteristic time.

If the attractive part is not deep enough, one expects that the event of aggregation of two clusters can be followed by reorganization (restructuring) or dissociation of the aggregates. In the latter case the irreversible character of the process is lost and one is led to deal with iii) *reversible* CCA. The properties of cluster-cluster aggregates are also affected by the kind of motion

they undergo. The trajectory of a cluster can be Brownian or ballistic. In addition, the clusters may rotate. Many of these processes have been studied by the three main approaches (simulations, theory and experiments) to be discussed in this section.

8.1. STRUCTURE OF CLUSTER-CLUSTER AGGREGATES

Both the related experiments and simulations indicate that cluster-cluster aggregates are typically highly ramified, almost loopless structures exhibiting fractal properties. In contrast to off-lattice DLA clusters, the overall shape of cluster-cluster aggregates is not spherical. Instead, these aggregates can be characterized by a well defined *asphericity* which becomes more pronounced as the clusters become larger (Medalia 1967). This fact is a trivial consequence of the growth mechanism: the overall shape can not be spherical since joining two spherical clusters would immediately destroy the symmetry. In contract to their overall shape, however, the density correlations within cluster-cluster aggregates are isotropic (Kolb 1985).

The fractal dimension of CCA clusters can be determined by the application of methods discussed in Chapter 4. For aggregates generated by Monte Carlo simulations, the power law decay of the density-density correlation function (Eq. (2.14)), the dependence of the radius of gyration on the mass of the aggregates (4.12) or the scaling assumption (4.14) can be used to evaluate D.

8.1.1. Fractal dimension from simulations

The actual realization of a cluster-cluster aggregation model in the computer depends on the particular process to be simulated. However, the most widely used simulations are based on the following assumptions. The particles are represented by occupied sites of a d-dimensional hypercubic cell of linear size L. To make the finite-size effects smaller, periodic boundary conditions are used. Initially, $N_0 = \rho L^d$ sites are randomly filled, where $\rho \ll$

1 is the density of the particles in the system. Then the clusters are allowed to move following Brownian or ballistic trajectories. If during their motion two or more particles belonging to different clusters accidentally occupy adjacent (nearest neighbour) sites, the clusters combine to form a single new aggregate with a probability $0 < p_s \leq 1$.

In *diffusion-limited cluster-cluster aggregation* (Meakin 1983c, Kolb *et al* 1983) the clusters are assumed to undergo random walks on the lattice, and $p_s = 1$. The mobility of the clusters is presumed to depend on the number of particles s they are made of. In particular, it is assumed that the diffusion coefficient D_s of a cluster of size s is given by

$$D_s = Cs^{\gamma}, \tag{8.1}$$

where C is a constant and γ can be used to take into account the effects of cluster geometry. For example, in a typical physical system one expects that $\gamma \simeq -1/D$, because the mobility of a cluster in a fluid is inversely proportional to its hydrodynamic radius which for an aggregate of fractal dimension D is close to to its linear extension (e.g. de Gennes 1979). For the case $\gamma = 0$, corresponding to a mass-independent diffusion coefficient, clusters are selected randomly and moved by one lattice unit in a direction chosen randomly from the $2d$ possible directions. If $\gamma \neq 0$ the following procedure is used to decide which of the clusters should be moved next. A random number r uniformly distributed in the range $0 \leq r \leq 1$ is selected and the cluster is moved only if $r < D_s/D_{max}$, where D_s is the diffusion coefficient of the given cluster and D_{max} is the largest diffusion coefficient for any cluster in the system.

The above lattice model can be generalized to the off-lattice case in a manner analogous to that used to simulate off-lattice DLA (Section 6.1.1). Similarly to diffusion-limited aggregation, this modification is not expected to change the fractal dimension of the clusters (Meakin 1987b). Fig. 8.2 shows the projection of an off-lattice diffusion-limited cluster-cluster aggregate embedded into three dimensions. Since this projection is not space filling, the fractal dimension of the aggregate itself should be less than 2 (see

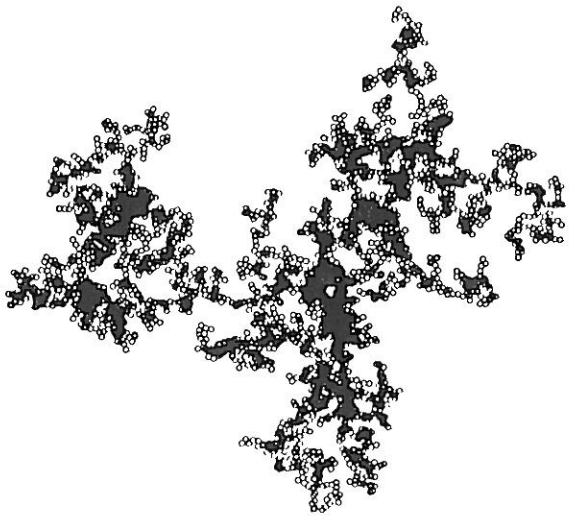

Figure 8.2. Projection of an off-lattice diffusion-limited CCA cluster grown in a three-dimensional simulation (Meakin 1987b). Comparison of this figure with Fig. 8.14 shows the relevance of computer simulation results to the experiments.

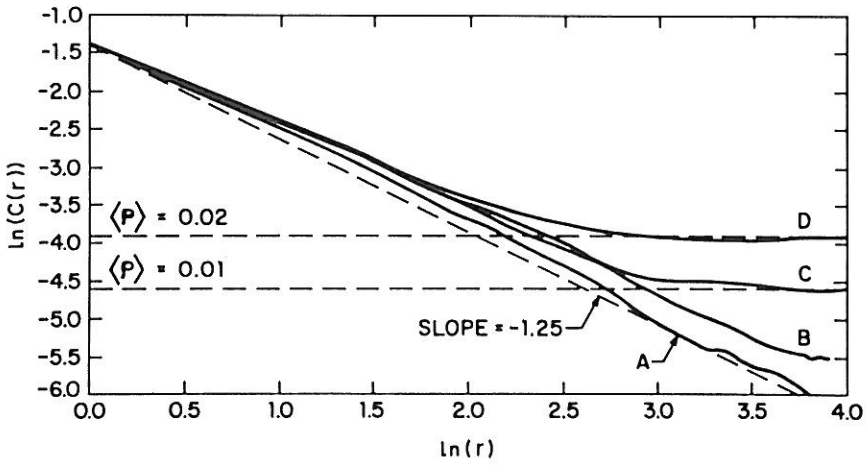

Figure 8.3. Dependence of the density correlations within diffusion-limited CCA clusters on the interparticle distance r. The crossover to the non-fractal behaviour is indicated by the horizontal part of the curves (Meakin 1987b).

rule a) of Section 2.2.).

One way to investigate the structure of aggregates is to calculate the density-density correlation function $c(r)$ given by (2.14) (Meakin 1987b). In

addition to the determination of the fractal dimension, this method can also be used to study the effects of finite constant density of particles ρ. Results for $c(r)$ obtained from three-dimensional simulations of CCA are displayed in Fig. 8.3. For $r < r_c$ the plot of $\ln c(r)$ versus $\ln r$ is approximately a straight line with a slope $\alpha = D - d$, where r_c is a ρ-dependent crossover scale. The power law decay of $c(r)$ indicates that the density distribution within the aggregates has a fractal scaling up to r_c. In the vicinity of the crossover scale this behaviour is changed, and for $r > r_c$ the correlation function becomes approximately constant. Such a crossover corresponds to a structure which is homogeneous on length scales larger than r_c. To estimate r_c one assumes that the large network spanning the whole cell at the final stage of the simulation is made of fractal subunits of dimension D. The number of subunits is proportional to N_0/r_c^D. Since the network fills the cell of volume L^d more or less homogeneously, and the effective volume occupied by a subunit is r_c^d, we can write

$$L^d \sim \frac{N_0}{r_c^D} r_c^d. \tag{8.2}$$

From the above expression one obtains

$$r_c \sim \rho^{D-d} \sim \rho^{-\alpha}, \tag{8.3}$$

where $\alpha = d - D$ is the codimension (2.18) and $\rho = N_0/L^d$.

The d-dependence of the fractal dimension of aggregates grown by diffusion-limited CCA is presented in Table 8.1. Clearly, these aggregates have a considerably smaller D than DLA clusters generated on lattices of the same dimension. This result is quite plausible; individual particles can penetrate a DLA cluster easily enough to increase its dimension to at least $d - 1$ (6.4). Cluster-cluster aggregates do not tend to fill holes within each other, being fractal structures themseves. The values obtained for the $d = 2$ and $d = 3$ cases are in good accord with the experimental results discussed in Section 8.3.1.

The question of the dependence of D on the diffusivity exponent γ

Table 8.1. Dependence of the fractal dimension of diffusion-limited cluster-cluster aggregates on d as determined from the correlation function (D_α) and from the radius of gyration (D_ν).

d	D_α	D_ν	N_{max}
2	1.44±0.03	1.43±0.02	$\sim 10^4$
3	1.78±0.06	1.75±0.01	$\sim 10^4$
4	2.12±0.10	2.03±0.04	$\sim 10^4$
5	–	2.21±0.02	$\sim 10^3$
6	–	2.38±0.02	$\sim 10^3$

arises naturally. The simulation carried out in two dimensions suggests that for $\gamma < 1$ the aggregates have approximately the same fractal dimension $D \simeq 1.45$. However, it is clear that in the limit of $\gamma \gg 1$ and low concentration CCA should become equivalent to DLA, as in this case practically only a single cluster (the largest one) is moving and it collects the rest of the individual particles during its diffusional motion. The behaviour of the density-density correlations in clusters obtained at the end of the simulations for various γ indicates a continuous change in the fractal dimension from a value of $D \simeq 1.45$ for $\gamma = 0$ to $D \simeq 1.7$ for $\gamma = 2$ (Meakin 1985c). Therefore, if $\gamma > 2$ the dimension of cluster-cluster aggregates is the same as that of DLA clusters. The nature of the *crossover* from CCA to DLA is not completely understood. The above mentioned simulations suggest a continuous change between the two regimes, while theoretical considerations imply a sudden jump from one type of behaviour into the other one as a function of γ.

Models for *reaction-limited cluster-cluster aggregation* (Jullien and Kolb 1984, Brown and Ball 1985) are constructed to represent the zero sticking probability limit of CCA. If $p_s \simeq 0$, each of the possible contact configurations of two clusters has the same probability to occur. This model is a cluster-cluster analogue of the particle-cluster model of Eden (1961), where each surface site is filled with equal probability. While for the Eden model $D = d$, in the case of reaction-limited CCA because of obvious steric

constraints, the clusters can not become compact.

A possible realization of reaction-limited CCA on cubic lattices is based on placing two clusters at random positions in a large cell. The resulting configuration is accepted as a new cluster only if the two clusters are adjacent and do not overlap. There are two main possibilities for chosing the above two clusters. i) To produce a *monodisperse* size distribution (Jullien and Kolb 1984) one starts with 2^n monomers. At each iteration a dimerization is made until there are no monomers left. Next the dimers are joined to form clusters of 4 particles and so on. ii) In the *polydisperse* case (Brown and Ball 1985) the clusters are always randomly selected from the ones available at the given stage.

Based on the results for the fractal dimension, the monodisperse and the polydisperse cases are principally different. The following values were obtained

$$D = 1.53 \pm 0.01 \quad (d = 2) \quad \text{and} \quad D = 1.94 \pm 0.02 \quad (d = 3) \tag{8.4}$$

for the monodisperse distribution and

$$D = 1.59 \pm 0.01 \quad (d = 2) \quad \text{and} \quad D = 2.11 \pm 0.03 \quad (d = 3) \tag{8.5}$$

for the polydisperse system. It is clear from the above expressions that D is larger for these models than it is for diffusion-limited CCA. This is well illustrated by the most important three-dimensional case for which $D \simeq 1.75$ in the diffusion-limited and $D \simeq 2.11$ in the reaction-limited version of cluster-cluster aggregation, in good agrement with the experimental results.

A relevant quantity associated with reaction-limited CCA is the number of ways C_{s_1,s_2} in which cluster 1 and cluster 2 can be positioned adjacent to each other. The square root of this quantity for $s_1 = s_2 = s$ gives an estimate of the number of active sites (sites at which a contact can be made) of an s particle cluster. The simulations indicate that the average value of the active sites scales as (Jullien and Kolb 1984)

$$\langle C_s^{1/2} \rangle \sim s^{\delta}. \tag{8.6}$$

For the monodisperse case $\delta \simeq 0.37$ $(d = 2)$, $\delta \simeq 0.58$ $(d = 3)$ and $\delta \simeq 0.72$ $(d = 4)$ were found to give the best fit to the data. It is obvious that δ must be smaller than 1 since only a fraction of the particles of a cluster is accessible when two aggregates are probed for contact. However, at the upper critical dimension d_c (if it exists) we expect $\delta = 1$, because for $d \geq d_c$ the aggregates are transparent to each other (see next Section).

In the off-lattice *ballistic cluster-cluster aggregation* model (Sutherland 1967) clusters are combined in pairs without the presence of other clusters (i.e., in the zero concentration limit). The process is started with a list of hyperspherical particles. During the simulation, particles or clusters are picked from the list in a stochastic manner, rotated to a random orientation, and are combined via randomly selected straight trajectories to form a larger cluster. The two clusters are joined at the point of first contact. After the new cluster has been formed, it is returned to the list, while the two precursors are erased. This process is continued until a single large cluster is obtained.

The clusters can be selected from the list according to a probability depending on some characteristics of the aggregates. As was discussed for reaction-limited CCA, one possibility is i) to pick a cluster completely *randomly* (polydisperse case). In the ii) *hierarchical models* (e.g. Sutherland 1967, Jullien and Kolb 1984) only clusters of the same size are joined. In this case the simulation starts with 2^k particles which are combined to form 2^{k-1} binary clusters (monodisperse size distribution). iii) An additional possibility is to choose a cluster with a *probability* depending on its *size*, e.g., in the form (8.1). In this model the probability of choosing two clusters of masses s_1 and s_2 simultaneously is proportional to $(s_1 s_2)^{\gamma}$.

Simulations of off-lattice ballistic aggregation corresponding to cases i) and ii) resulted in practically unchanged fractal dimensions for a given d (Meakin 1987b). For $d = 2$ and $d = 3$ the values $D \simeq 1.55$ and $D \simeq 1.91$ were obtained, respectively. These numbers are closer to the fractal dimension of

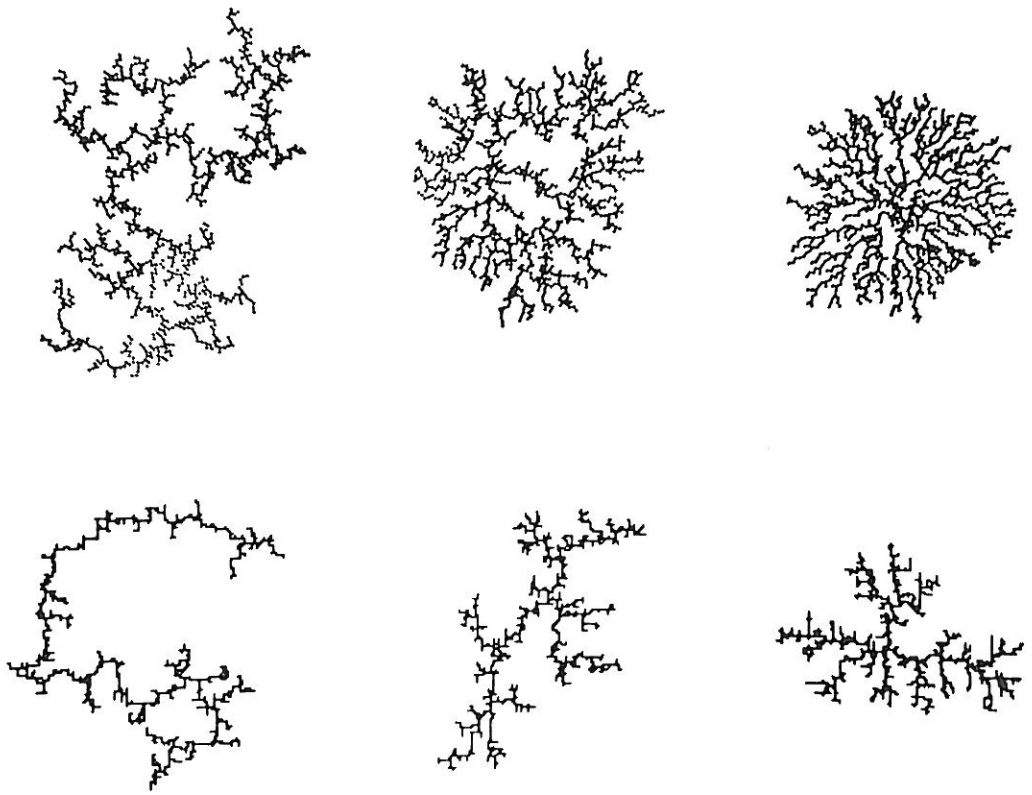

Figure 8.4. Crossover from CCA to ballistic particle-cluster aggregation as a function of γ when the objects move along straight line trajectories (upper row). In the diffusion-limited case the process crosses over to DLA for large γ (Jullien *et al* 1984).

reaction-limited CCA clusters than to that determined for diffusion-limited cluster-cluster aggregates. Model iii) provides a possibility to demonstrate the effects of cluster mobility. In Fig. 8.4 (upper row) the crossover from CCA to particle-cluster ballistic aggregation-type structures is illustrated. In the diffusion-limited case a crossover from CCA to DLA can be seen (lower row) occurring in this approach at $\gamma = 1$.

In all of the CCA models discussed above it was assumed that the density of particles in the system is much less than unity. However, it is of interest to consider what happens for ρ close to 1. The $\rho = 1$ limit can be investigated using the following procedure (Kolb and Herrmann 1987). Initially, one particle is placed on each site of the square lattice. The particles try to move in a randomly selected direction, and form a cluster (establishing a bond) with the particle they would collide with (clusters also try to move

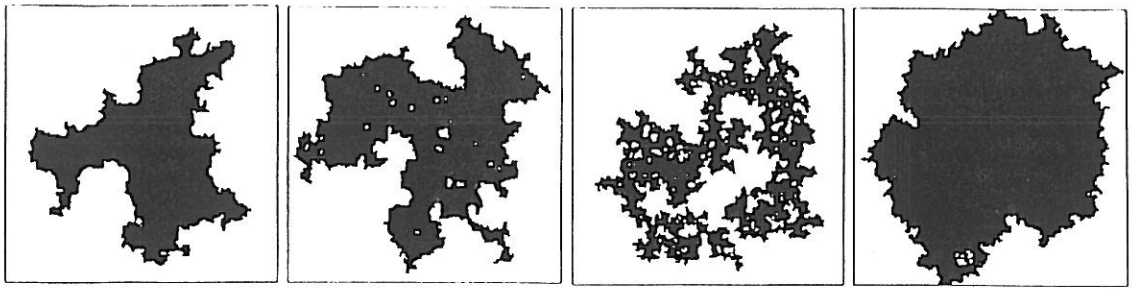

Figure 8.5. Clusters generated in the simulations of high density CCA. In these numerical experiments both surface and volume fractals could be observed. The first picture (from left) shows a non-fractal cluster having a fractal surface ($\gamma = -2$), while the third configuration represents a fractal cluster ($\gamma = 1$).

and are combined with those they would hit). Therefore, the clusters are defined as sets of particles connected by permanent bonds formed during their attempts to move. A cluster is selected for a trial jump with a frequency given by (8.1). The results are demonstrated in Fig. 8.5. Depending on γ the following structures can be observed just before the linear size of the largest cluster becomes comparable to that of the cell: a) Compact clusters with fractal surface ($\gamma = -2$), b) fractal aggregates ($\gamma = 1$), and c) non-fractal objects ($\gamma = 2$).

There are many more variants of cluster-cluster aggregation. A number of them lead to fractal dimensions different from the ones given above for the basic models. Non-universality was observed, for example, in ballistic CCA with a zero impact parameter (Jullien 1984) and in chain-chain diffusion-limited aggregation (Debierre and Turban 1987), where branching is not allowed.

8.1.2. Theoretical approaches

Before presenting a few theoretical results, it has to be pointed out that there is no standard theory for the fractal dimension of cluster-cluster aggregates. The theoretical methods well founded to determine the scaling

behaviour in equilibrium phenomena are not applicable to diffusion-limited CCA because of its far from equilibrium nature. The situation is similar to the case of other growth processes such as DLA. However, unlike diffusion-limited aggregation, CCA can be shown to have an *upper critical dimension.* This is perhaps the most important result obtained for cluster-cluster aggregates by theoretical arguments.

To treat CCA theoretically we consider the following "Sutherland's Ghost" model (Ball and Witten 1984b). Let us imagine that the clusters are constructed according to an algorithm similar to the hierarchical version of the ballistic aggregation model (previous Section). However, instead of combining the clusters using ballistic trajectories, one selects a monomer belonging to each of the two clusters, and joins the clusters by positioning these monomers on adjacent sites of the lattice (this is done in the spirit of reaction-limited CCA). The specific feature of this model is that the particles are *allowed to overlap.*

The fractal dimension of such clusters can be calculated by determining the average number of bonds $b(2s)$ (chemical distance) separating one particle from another on an aggregate consisting of $2s$ particles. If two particles are chosen at random on a $2s$-site cluster, the probability that they both belong to the A cluster or both belong to the B cluster is equal to $1/4$, where A and B denote the two s-site constituent clusters. In this case the average number of bonds is $b(s)$. With a probability $1/2$ one of the two chosen particles belongs to A, the other one to B. Then the path on A to the contact point, and on B from this point to the other chosen particle add up on average to give $2b(s)$. The three cases together give $b(2s) = 3/2b(s)$ which means that $b(s) \sim s^{\ln(3/2)/\ln 2}$. It follows from the construction (clusters of independent orientations are linked, and no overlaps occur) that the shortest path connecting two particles on the cluster behaves as a random walk (Section 5.3.1). Thus one has for the mean square distance between the particles $R^2 \sim b(s)$. From here it follows (Ball and Witten 1984b) that $s \sim R^D$ with

$$D = D_c = 2\frac{\ln 2}{\ln 3/2} \simeq 3.4. \tag{8.7}$$

The above fractal dimension (which is independent of d) was obtained by letting the clusters interpenetrate freely. This crude approximation can be improved by modifying the model to take into account self-avoidance or excluded volume effects. This can be done in a computer by discarding overlapping configurations. The obtained hierarchical model is identical to reaction-limited CCA discussed above. However, if

$$2D - d < 0, \tag{8.8}$$

only a small fraction of the configurations have to be removed and the two models become equivalent. Condition (8.8) is related to rule f) discussed in Section 2.2. giving the fractal dimension of the intersection of two fractals. If (8.8) is satisfied, the intersection has a fractal dimension equal to zero, consequently, overlaps occur with a probability less than 1. Therefore, excluded volume effects are negligible in embedding dimensions above $d_c = 2D_c \simeq 6.8$, which can be regarded as the upper critical dimension of reaction-limited cluster-cluster aggregation in analogy with d_c for ordinary equilibrium systems.

In fact, *reaction-limited* CCA can be considered as an *equilibrium* model since the various clusters appear with the same probability (Witten 1985). One expects that this model is closely related to lattice animals. Lattice animals are the collection of all possible connected configurations on a lattice consisting of a given number of sites taken with equal weight. The main difference between the two ensembles is that the former one is a subset of lattice animals corresponding to binary decomposable configurations. For equilibrium systems the heuristic Flory theory gives up to $d = d_c$

$$D = \frac{d+2}{2(1+1/D_c)}, \tag{8.9}$$

where D_c is the fractal dimension of clusters in d_c-dimensional space. If $d \geq d_c$, $D = D_c$. For lattice animals $D_c = 4$, and the critical dimension is $d_c = 8$. Substituting $D_c = 3.4$ into the above expression one gets the estimates for the fractal dimension of monodisperse reaction-limited aggregates $D \simeq 1.55$

($d = 2$) and $D \simeq 1.93$ ($d = 3$) in surprisingly good agreement with the simulation results (8.4).

For *diffusion-limited and ballistic* CCA similar arguments can be used to obtain the upper critical dimension. Again, two particles can be used to link together two aggregates, but the obtained configuration has to be discarded if letting one of the clusters undergo a random walk results in an overlap during its diffusional motion (for the ballistic case straight line trajectories have to be considered). The effective dimension of the object consisting of the sites visited by the diffusing aggregate of dimension D is $D + 2$, since this object can be obtained by replacing each particle by a random walk of dimension 2. Consequently, for diffusion-limited CCA $d_c = 2D_c + 2 \simeq 8.8$. For the ballistic case we have $d_c = 2D_c + 1 \simeq 7.8$ (Witten 1985). In general, one expects that a higher upper critical dimension results in a lower fractal dimension for a given $d < d_c$. The numerical results are in good agreement with the above critical dimensions, because for a fixed d they satisfy $D_d(\text{diff.lim}) < D_d(\text{ballistic}) < D_d(\text{react.lim.})$.

8.2. DYNAMIC SCALING FOR THE CLUSTER SIZE DISTRIBUTION

The fractal dimension conveys information about the static or geometrical properties of a single aggregate. However, in a typical cluster-cluster aggregation process there are many clusters simultaneously present in the system, and the evolution of this ensemble of aggregates is of interest as well. This time dependence can be investigated by determining the *dynamic cluster-size distribution function* $n_s(t)$, which is the number of clusters in a unit volume consisting of s particles at time t.

The study of the statistics of clusters is a common approach to the description of ensembles of clusters. In many equilibrium systems n_s is known to decay as a power law at the critical point. Analogously, $n_s(t)$ has been shown to exhibit static (as a function of s) and dynamic (as a function of t) scaling in a number of close-to or far-from equilibrium systems (Binder 1976). In this Section we first treat computer simulations of the diffusion-limited and related cluster-cluster aggregation models together with the dynamic scaling

picture emerging from these numerical investigations. This will be followed by a discussion of the mean-field Smoluchowski (1917) equation.

8.2.1. Diffusion-limited CCA

In the diffusion-limited cluster-cluster aggregation model (Section 8.1.1.) the clusters move along Brownian trajectories and stick together on contact. Initially there are $N_0 = \rho L^d$ monomers in a cell of linear size L. To make the cluster size distribution function independent of the cell size we use the definition $n_s(t) = N_s(t)/L^d$, where $N_s(t)$ is the number of s-clusters at time t in the cell. The elapsed time is measured by increasing t by an amount Δt each time a cluster is selected to move.

The dynamic scaling of $n_s(t)$ can be well demonstrated simulating the simple version of CCA on a square lattice with mass independent cluster mobility corresponding to $\gamma = 0$ in (8.1). In this case $\Delta t = 1/n(t)$ has to be used to provide a physical time, where $n(t)$ is the normalized total number of clusters in the system at time t. The choice $\Delta t = 1$ would result in an unphysical acceleration with growing t (since $n(t) \to 0$ for $t \to \infty$, and this would lead to an increase of the number of steps per cluster per unit time). The expression $\Delta t = 1/n(t)$ yields the same diffusion coefficient for each cluster, and it corresponds to the Monte-Carlo step per spin type time definitions common in equilibrium simulations.

The results of simulations are illustrated in Figs. 8.6. Fig. 8.6a shows the dynamic cluster-size distribution as a function of s for fixed times, while $n_s(t)$ as a function of t is plotted in Fig. 8.6b for three selected values of the cluster size s. These simulations were carried out with $L = 400$ and initial particle density $\rho = 0.05$. There are a few important conclusions which can be drawn from these figures. i) The straight lines in Fig. 8.6a correspond to a power law decay of the cluster-size distribution as a function of s up to a cutoff value. This behaviour is analogous to that observed for equilibrium systems close to the critical point. However, for diffusion-limited CCA the exponent τ describing the decay of $n_s(t)$ with s, is smaller than 2, in contrast to equilibrium systems, where $\tau > 2$. ii) The position of the cutoff diverges

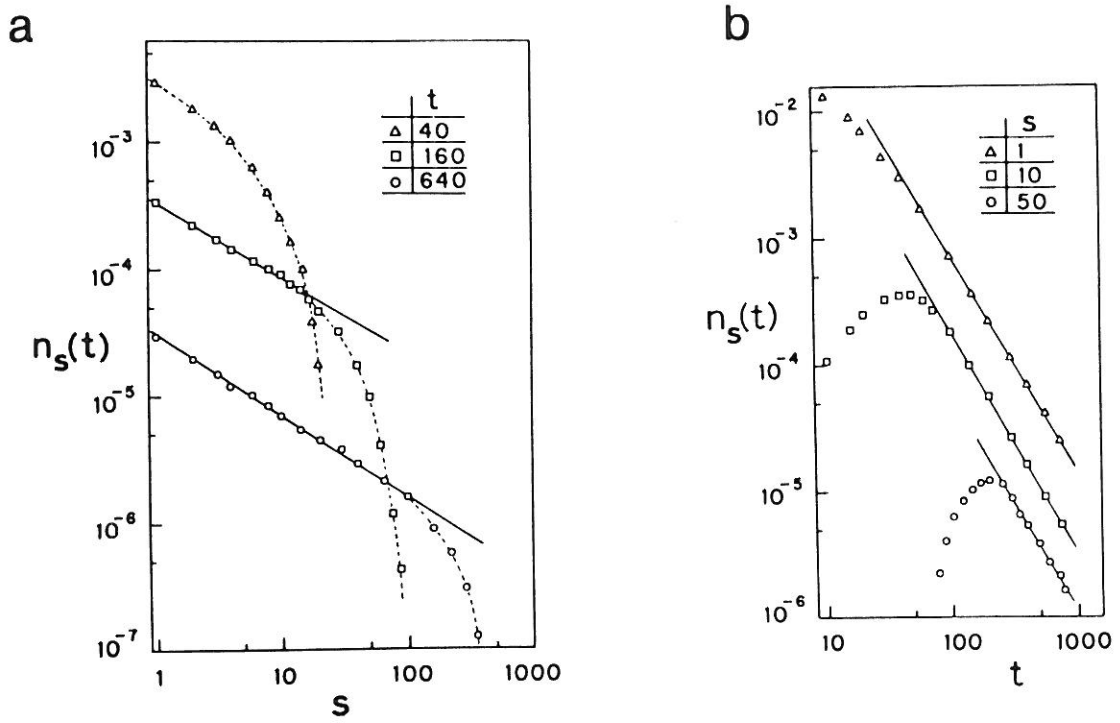

Figure 8.6. (a) Dependence of the dynamic cluster-size distribution function $(n_s(t))$ on the number of particles in the clusters $(s)$for fixed times (t). (b) $n_s(t)$ as a funcion of time for three selected values of s (Vicsek and Family 1984).

with t. iii) According to Fig. 8.6b, $n_s(t)$ scales as a function of t (for fixed s) as well.

These observations can be well represented by the *scaling assumption* (Vicsek and Family 1984a,Kolb 1984)

$$n_s(t) \sim s^{-\theta} f(s/t^z), \tag{8.10}$$

where θ and z are constants analogous to critical exponents, and $f(x)$ is a scaling function. $f(x)$ is such that $f(x) \ll 1$ (it is exponentially small), if $x \gg 1$ and $f(x) \sim x^{\delta}$, if $x \ll 1$ with δ usually called the crossover exponent. The above expression can be written in an alternative form which contains the scaling of $n_s(t)$ as a function of s and t *explicitly* for small s/t^z

$$n_s(t) \sim t^{-w} s^{-\tau} \tilde{f}(s/t^z), \tag{8.11}$$

where the cutoff function is approximately a constant for $x \ll 1$ and decays faster than any power law as $x \to \infty$. The term t^{-w} corresponds to a process typical for cluster-cluster aggregation; the clusters which are much smaller than s/t^z gradually die out forming larger aggregates. The characteristic cluster size is determined by the denominator t^z.

The scaling assumption (8.11) and the normalization condition

$$\rho = \sum_{s=1}^{\infty} n_s(t)s \sim \int_1^{\infty} n_s(t)s ds \tag{8.12}$$

can be used to obtain a scaling relation among the exponents w, z and τ. Inserting (8.11) into (8.12) we have

$$\rho \sim t^{-w} \int_1^{\infty} s^{1-\tau} f(s/t^z) ds \sim t^{-w+(2-\tau)z} \int_{t^z}^{\infty} x^{1-\tau} f(x) dx. \tag{8.13}$$

From (8.13) it follows that (Vicsek and Family 1984a)

$$w = (2-\tau)z, \tag{8.14}$$

since $0 < \rho < 1$ when $t \to \infty$ and the last integral is a constant in the same limit. Obviously, $\tau < 2$ has to be satisfied, because in a physical system $w, z > 0$.

The *mean cluster size* $S(t)$ diverges for $t \to \infty$. Expressing $S(t)$ through $n_s(t)$, and using (8.11) and (8.14) we get

$$S(t) = \frac{\sum_s n_s(t)s^2}{\sum_s n_s(t)s} \sim t^z. \tag{8.15}$$

Similarly, for the *total number of clusters* in the system, $n(t) = \sum_s n_s(t)$ one has (Vicsek and Family 1984b)

$$n(t) \sim \begin{cases} t^{-z}, & \text{if } \tau < 1 \\ t^{-w}, & \text{if } \tau > 1. \end{cases} \tag{8.16}$$

Thus the scaling of the total number of particles in time is determined by the value of the exponent τ. The simulations in $d = 2$ resulted in the estimates $w \simeq 1.7$, $z \simeq 1.4$ and $\tau \simeq 0.7$.

For $x \ll 1$ (8.10) can be written in the form $n(t) \sim t^{-z\delta} s^{-\theta+\delta}$. Comparing this with (8.11) one obtains $w = z\delta$ and $\theta - \delta = \tau$. Because of the scaling relation (8.14), from here it follows that in (8.10)

$$\theta = 2. \tag{8.17}$$

The mass dependent cluster mobilities of the form (8.1) strongly influence the dynamics as well. These effects were investigated by simulating diffusion-limited CCA in two and three dimensions (Meakin *et al* 1985). To provide cluster mobilities proportional to s^{γ} one can use the following procedure. i) First a cluster is selected randomly. ii) Then a random number p distributed uniformly on the unit interval is generated, and the given cluster is moved in a random direction by one lattice unit only if $p < D_s/D_{max}$, where D_s is the diffusion coefficient of the selected cluster and D_{max} is the largest diffusion coefficient for any cluster in the system. iii) Finally, on each occasion when a cluster is chosen the time is incremented by $\Delta t = 1/[n(t)D_{max}]$ even if the cluster is not moved. In other words the time is incremented by Δt for each attempted move.

The dependence of the exponents w, z and τ on γ can be determined from log-log plots of the quantities $S(t)$, $N(t) = n(t)L^d$ and $N_s(t)$ for various γ. The results obtained from three-dimensional simulations are summarized in Table 8.2. This Table shows that for γ smaller than some critical γ_c the shape of the cluster-size distribution function changes qualitatively. If $\gamma < \gamma_c$, $n_s(t)$ does not decay as a power law for small s, and in the scaling law (8.11) $w = 2z$.

Thus the behaviour of $n_s(t)$ is *non-universal* as a function of γ. For $\gamma > 0$ the large clusters move faster, and relatively many small ones do not take part in the aggregation process. In this case $n_s(t)$ is characterized by many small clusters and a gradually decreasing number of clusters for growing sizes. If $\gamma < 0$, the small clusters have a higher velocity, so they die

Table 8.2. Exponents τ, w and z obtained from three-dimensional simulations of diffusion-limited CCA for various values of the diffusivity exponent γ. Note that the scaling theory predicts $w = (2-\tau)z$ for $\gamma > \gamma_c$ and $w = 2z$ for $\gamma < \gamma_c$.

γ	z	w	τ
-3	0.33	0.64	
-2	0.45	0.90	
-1	0.85	1.60	
-1/D	1	2.2	
-1/2	1.3	2.6	$\simeq 0$
0	3	2.2	1.3
1/2	~ 100	12	1.87

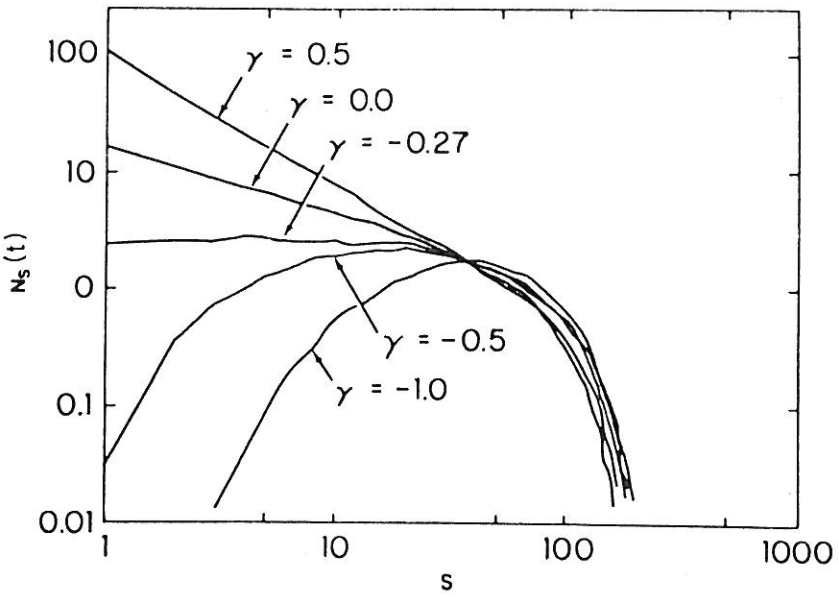

Figure 8.7. Cluster-size distribution functions obtained from simulations of diffusion-limited CCA on the square lattice. As γ is decreasing, at a critical value of the diffusivity exponent $\gamma_c \simeq -0.27$, the monotonic decay of the distribution crosses over into a different, bell-shaped behaviour (Meakin *et al* 1985).

out (aggregate) quickly, forming larger clusters. Thus there will be only a few small and very large clusters in the system, resulting in a non-monotonic, bell-shaped distribution.

The *crossover* between the monotonic and the bell-like behaviour occurs at some γ_c depending on d (Meakin *et al* 1985). For example, in $d = 2$ this qualitative change in $n_s(t)$ occurs near $\gamma_c \simeq -0.27$. This is demonstrated in Fig. 8.7. According to Table 8.2, in three dimensions $\gamma_c \simeq -0.5$. On the other hand, one expects that the mobility of clusters in a fluid is inversely proportional to their hydrodynamic radius. The latter scales the same way as the radius of gyration of the clusters, thus $D_s \sim 1/R_s \sim s^{-1/D}$, where $1/D \simeq 0.57$. Consequently, in $d = 3$ the critical mobility exponent γ_c is just in the range where γ is likely to be in a real system in which the diffusion process is controlled by shear viscosity.

The above discussed results for the dynamics of diffussion-limited cluster-cluster aggregation can be summarized as follows. The cluster-size distribution is described by dynamic scaling of the form

$$n_s(t) \sim s^{-2} f(s/t^z), \tag{8.18}$$

where $f(x)$ depends on the mobility exponent γ. In particular,

$$f(x) \sim x^2 g(x) \qquad \text{for} \quad \gamma < \gamma_c \tag{8.19}$$

with $g(x)$ exponentially small for both $x \ll 1$ and $x \gg 1$, and

$$f(x) \sim \begin{cases} x^\delta, & \text{if } x \ll 1 \\ \ll 1, & \text{if } x \gg 1 \end{cases} \qquad \text{for} \quad \gamma > \gamma_c. \tag{8.20}$$

The scaling (8.18) can be checked by plotting the quantity $s^2 n_s(t)$ as a function of s/t^z. If (8.18) is valid, then the results obtained for a given γ should fall onto a single curve corresponding to the scaling function $f(x)$. Fig. 8.8 demonstrates that for the simulations carried out in $d = 3$ with $\gamma = -2$ this is indeed the case.

The *region of validity* of the dynamic scaling (8.18) depends on the parameters of the problem. Equation (8.18) is expected to describe the evolution of the process in the limit when the particle density is small ($\rho \ll 1$).

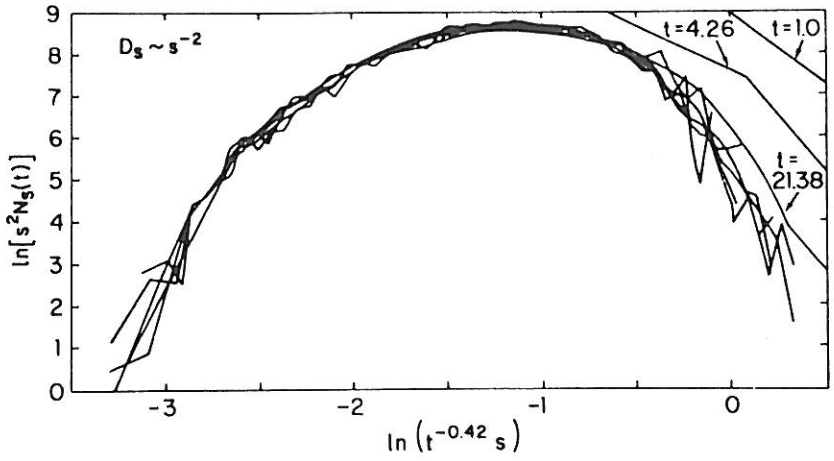

Figure 8.8. Scaling of the dynamic cluster-size distribution function. (8.18) is supported by the fact that after a relatively short time the data determined for various times fall onto a single curve. In these three-dimensional simulations $\gamma = -2$ was used (Meakin *et al* 1985).

In addition, $s \gg 1$ and $t \gg 1$ are required in order to be in the scaling region.

For the time variable, however, there is an *upper bound* as well, for the following reasons. First, in a finite system the total number of clusters $N(t)$ after some time becomes so low that a statistical interpretation of the cluster size distribution loses its meaning. Second, a non-trivial crossover is expected to occur at a time t_g depending on the particle density ρ. As the aggregation process goes on, the number of clusters decreases and, correspondingly, the average number of particles in the clusters, $\bar{s}(t)$, increases. Assuming that the clusters are approximately of the same size (this is so for $\gamma < \gamma_c$) the average cluster radius grows in time as $\bar{R}(t) \sim [\bar{s}(t)]^{1/D} \sim [\rho/n(t)]^{1/D} \sim t^{z/D}$. In contrast, the average distance between the centres of two clusters, $\bar{r}(t)$, grows as $\bar{r}(t) \sim [n(t)]^{-1/d} \sim t^{z/d}$, i.e., slower, because $d > D$. This means that approaching the time t_g at which $\bar{R}(t)$ becomes as large as $\bar{r}(t)$, the aggregation process crosses over into *gelation* and an infinite network (gel) appears. Naturally, in this limit the dynamic scaling (8.18) breaks down. Thus, diffusion-limited CCA is a suitable model to simulate gelation in colloidal systems.

The above qualitative picture can be made more quantitative (Kerstein

and Bug 1984) by using (8.18) for the determination of the effective volume, $V(t)$, occupied by the clusters. This is done by calculating

$$V(t) = \sum_s V_s n_s(t) \sim \rho \int_1^\infty s^{d/D-2} f(s/t^z) \sim \rho t^{(d/D-1)z}, \tag{8.21}$$

where $V_s = s^{d/D}$ is the effective volume occupied by an s-site cluster and the prefactor is chosen so that $V(1) = \rho$ (at the first time step V is equal to the volume fraction of the diffusing particles). Setting $V(t_g) = 1$, (8.21) gives the estimate

$$t_g \simeq \rho^{1/[z(1-d/D)]} \tag{8.22}$$

depending on ρ, D and z (where z itself depends on γ but it is always larger than zero). Accordingly, gelation occurs at finite time for every γ, although $t_g \to \infty$ as $\rho \to 0$. The gelation time becomes very large also for $\gamma \ll 0$ since in this case $z \ll 1$.

Dynamic scaling of the form (8.18-8.20) is a general property of many cluster-cluster aggregation processes in which the aggregates move along Brownian trajectories (Section 8.3.2.). The cluster-size distribution in a number of related computer models was found to follow (8.18), including chain-chain aggregation (Debierre and Turban 1987), the particle coalescence model and aggregation of anisotropic particles (Miyazima *et al* 1987).

8.2.2. Reaction-limited CCA

Reaction-limited cluster-cluster aggregation in the form introduced in Section 8.1.1. does not allow the investigation of dynamic properties because there is no physical time scale defined in the model. One way to study the dynamics of aggregation in realistic reaction-limited processes is to use the diffusion-limited CCA model with very small sticking probabilities (Family *et al* 1985b). The formation of a permanent bond between two clusters may depend on a number of parameters, including the mass of the two colliding

clusters. To be specific, in the following we shall describe the results of simulations with a sticking probability of the form

$$p_{s,s'} = p_0 s^{\sigma} s'^{\sigma}, \tag{8.23}$$

where s and s' denote the number of particles in the two clusters. In (8.23) $p_0 < 1$ and σ are constants and, naturally, if $p_0 s^{\sigma} s'^{\sigma} > 1$ one uses $p_{s,s'} = 1$. As before, the mobility of clusters depends on their size according to (8.1).

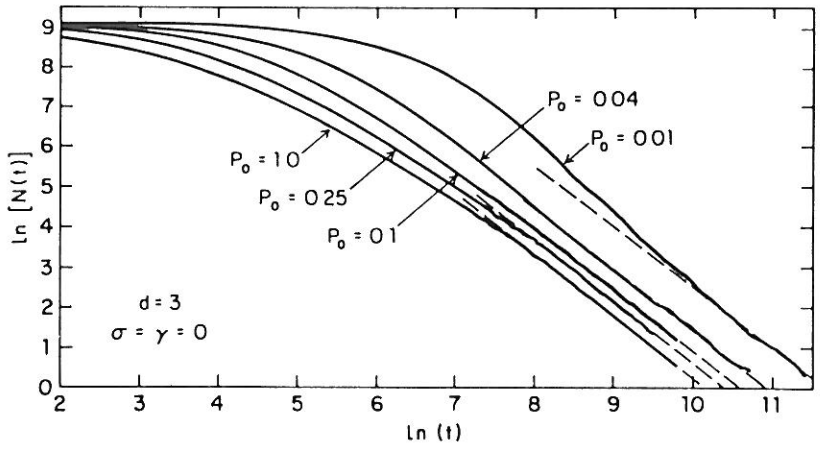

Figure 8.9. Time dependence of the total number of clusters in the three-dimensional cell for a fixed mass-independent sticking probability P_0 (Family *et al* 1985b)

Let us first consider the $\sigma = \gamma = 0$ case to study the effects of a small, mass-independent sticking probability p_0. The behaviour of the total number of clusters in the two-dimensional simulations is shown in Fig. 8.9. According to this figure, if $p_0 \ll 1$, at the beginning $N(t)$ decreases very slowly, but after a sufficiently long time it tends to zero as t^{-z}. The value of the exponent z is independent of p_0, and is about 1.5. This fact can be interpreted as the sign of a *crossover from reaction-limited into diffusion-limited* CCA. For short times there are only small clusters in the system. If they do not stick when colliding, there is a good chance that they diffuse away without coming into contact again. The number of clusters decreases slowly, the aggregation is reaction-limited. As the time increases, larger clusters are formed which can be linked in many ways and touch each other many times while they

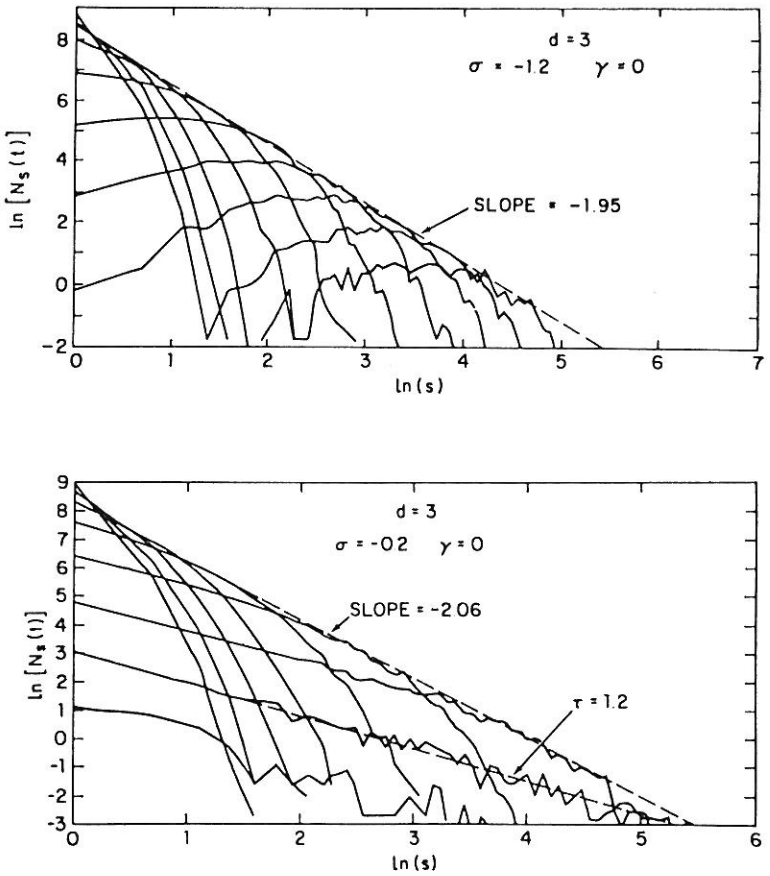

Figure 8.10. The cluster-size distribution function versus s for various times and for two selected values of the sticking probability exponent σ (Family *et al* 1985b).

are in the vicinity of each other. Thus if two large clusters get close, the probability that they stick becomes nearly 1, and the process crosses over into diffusion-limited aggregation.

Simulations with various values of the sticking probability exponent σ (Family *et al* 1985b) indicate that in analogy with the role of γ, changing σ may result in a qualitative change in the behaviour of the cluster-size distribution function $n_s(t)$. In particular, decreasing σ there exists a critical σ_c at which $n_s(t)$ crosses over from a monotonically decreasing into a bell-shaped distribution. This is demonstrated by Fig. 8.10. According to the simulations $\sigma_c \simeq -0.6$ in $d = 2$ and $\sigma_c \simeq -0.8$ in $d = 3$. Fig. 8.10 allows one to draw an additional conclusion. The envelope of the cluster-size distribution function for various times is a straight line (the common tangent) having a

slope approximately equal to -2. It can easily be shown that this has to be so if the time evolution of $n_s(t)$ is described by dynamic scaling of the form (8.18).

8.2.3. Steady-state and reversible CCA

The above discussed cluster-cluster aggregation models describe processes with a permanent evolution in time since the number of clusters in the corresponding systems is gradually decreasing. CCA models can be easily modified in order to simulate an important process of both practical and theoretical interest, in which a far-from-equilibrium steady-state distribution of clusters develops in the system. This can be accomplished by adding the following rules to those defining CCA: i) single *particles are fed* into the system and ii) simultaneously, clusters *are removed* according to some rules. In another approach the clusters are allowed to *break up*, and this process naturally leads to a time-independent, equilibrium cluster-size distribution.

Steady-state conditions are typical in many applied fields. For example, small smoke particles fed into the atmosphere form larger aggregates by coagulation. These aggregates disappear from the air by sedimentation due to the gravitational force. In the stirred tank reactors, often used for modelling chemical reactors in industry, an analogous process takes place but the particles are removed by letting them flow out from the chamber. In addition to the possible applications to engineering, steady-state coagulation is interesting from the theoretical viewpoint because of its analogy with dynamical critical phenomena in near equilibrium systems. Steady-state coagulation has been investigated by various approaches including experiments (Madelaine *et al* 1979), numerical methods (McMurry 1980), simulations (Vicsek *et al* 1985), and studies of the Smoluchowski equation approach (White 1982, Rácz 1985a).

One of the simplest models in which the scaling behaviour of steady-state aggregation can be investigated is the following. The process is the same as the original diffusion-limited CCA model, except that at every unit time kL^d particles are added to the system at different sites selected randomly,

where L is the linear size of the system and k is a small parameter. In addition, a cluster is discarded as soon as it becomes larger than a previously fixed number s_r. This latter rule is an extreme version of the situation in which larger clusters leave the system with a higher probability. In this way both the total number of clusters per unit volume, $n(t)$, and the number of particles in a unit volume, $m(t)$, in the system go to a k-dependent constant value (n_∞ and m_∞) for long times. The *relaxation time*, $t_r(k)$, corresponding to the characteristic time scale of the relaxation towards the steady-state is also expected to depend on the feed rate k.

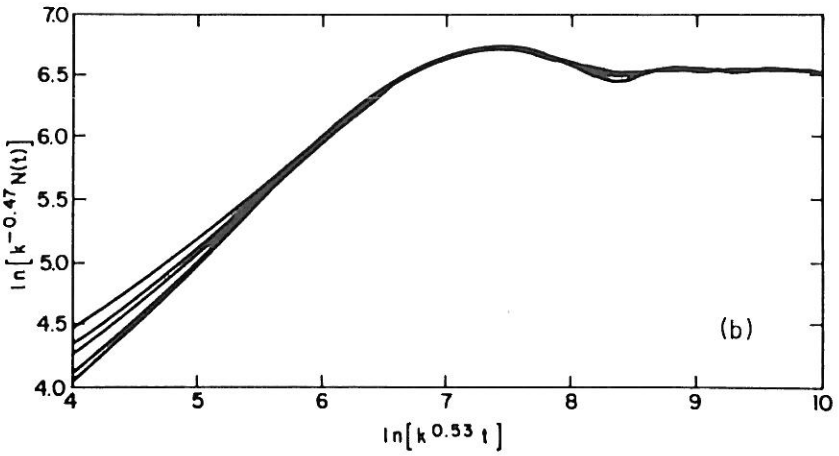

Figure 8.11. This figure shows how the scaling form (8.24) for the total number of clusters in the three-dimensional model of CCA with sources and sinks can be used to scale the data into a single function. The deviations from scaling apparent on the left-hand side of the plot is caused by the non-zero initial particle concentration used in the simulations (Vicsek *et al* 1985).

The results of the related simulations indicate that both the total number of clusters in the steady-state, n_∞, and the relaxation time, t_r, scale as a function of k. Correspondingly, for the case when $k \ll 1$ and the initial number of particles is very small the data for $n(t)$ can be well represented by the following *scaling form* for the number of clusters in the system at time t (Vicsek *et al* 1985)

$$n(t) \sim k^{\delta} f(k^{\Delta} t), \tag{8.24}$$

where $f(x)$ is a scaling function with $f(x) \sim x$ for $x \ll 1$ and $f(x) = 1$ for $x \gg 1$. The actual shape of $f(x)$ may depend on the parameters γ or s_r but for a fixed set of these numbers $n(t)$ can be expressed through the scaling form (8.24). The scaling behaviour represented by (8.24) is demonstrated in Fig. 8.11, where the $N(t)$ curves obtained in the three dimensional simulations for various feed rates are scaled into one universal function ($N(t)$ is the total number of particles in the L^d cell).

The values of the exponents δ and Δ can be determined from the slopes of the straight lines drawn through the data on the log-log plots of N_∞ and t_r versus k. It was found that in one dimension $\delta = 0.33 \pm 0.02$ and $\Delta = 0.65 \pm 0.03$. The two-dimensional simulations gave $\delta = 0.40 \pm 0.04$ and $\Delta = 0.58 \pm 0.05$ without, and $\delta = 0.52 \pm 0.04$ and $\Delta = 0.46 \pm 0.05$ with the logarithmic corrections taken into account, while in three dimensions $\delta = 0.47 \pm 0.05$ and $\Delta = 0.54 \pm 0.05$ were obtained.

The one-dimensional case can be treated both exactly and using an approximate rate equation for the number of clusters. Here we briefly discuss the latter approach because, in spite of its simplicity, the equation

$$\frac{dn(t)}{dt} = k - bn^3(t) - F(k, s_r, t) \tag{8.25}$$

reproduces the exact values for the exponents δ and Δ. In (8.25) b is a constant and the term $-F(k, s_r, t)$ describes the removal of clusters. The term $n^3(t)$ is included because of the following consideration. The rate of change of $n(t)$ due to coagulation is proportional to the number of clusters itself and to the average collision frequency of the clusters, ν. In one dimension, because of the diffusional motion, this frequency is inversely proportional to the square of the average distance X between the clusters. On the other hand, $X = 1/n(t)$, therefore, $\nu \sim n^2(t)$. Although the above arguments are not rigorous, they are quite plausible, and therefore (8.25) is expected to provide the right asymptotic behaviour of $n(t)$.

From (8.25) it can be seen that in the steady-state for $s \to \infty$ the number of clusters is equal to $(k/b)^{1/3}$, thus $\delta = 1/3$. In order to get an expression for the relaxation time one integrates (8.25) for $s_r \gg 1$. Keeping

only the term which becomes singular if $n(t) \to (k/b)^{1/3}$ we get from (8.25)

$$n(t) \simeq (k/b)^{\delta} - \lambda e^{-t/t_r}, \tag{8.26}$$

where the relaxation time is $t_r = k^{-\Delta}/3b^{1/3}$ with $\Delta = 2/3$ and $\delta = 1/3$. In (8.26), λ is a constant depending on the initial conditions. These values for δ and Δ satisfy the scaling law $\delta + \Delta = 1$ following from a scaling analysis of the Smoluchowski equation (next Section) and are in good agreement with the simulation results. A rigorous derivation (Rácz 1985b) using an analogy with the domain wall dynamics in the kinetic Ising model gives the same values for the exponents, but a different value for λ.

Having determined δ and Δ in $d = 1, 2$ and 3 we have the necessary data to discuss the question of the upper critical dimension for the dynamics of cluster-cluster aggregation under steady-state conditions. The simulations indicate scaling as a function of the feed rate with exponents $\delta = \Delta = 1/2$ for $d \geq 2$, if we assume the existence of logarithmic corrections in $d = 2$. Below two dimensions different values have been found. These results are consistent with an *upper critical dimension* $d_c = 2$ for the *kinetics* of steady-state CCA. In addition, the theoretical prediction $\delta + \Delta = 1$ is fulfilled for all cases considered.

Reversible cluster-cluster aggregation takes place if the bonds connecting the particles within a cluster can break. This is clearly a relevant process in a number of situations (e.g. Barrow 1981, Ziff and McGrady 1985, Ernst and van Dongen 1987); for example, as the clusters grow in size, the possibility of breakup increases. In reversible CCA coagulation decreases the number of clusters, whereas breakups increase $n(t)$. There exists a relaxation time t_r such that after a sufficiently long time, $t \gg t_r$, a balance is established between the two processes leading to an *equilibrium state* in which $n_s(t)$ is independent of time.

Let us consider the scaling behaviour of diffusion-limited CCA models in which the breakup probability for a particular bond that breaks the cluster of size $s = i + j$ into two clusters of masses i and j is

$$F_{ij} = h\Phi_{ij}, \tag{8.27}$$

where h is the breakup constant, Φ_{ij} is a function determining the dependence of the fragmentation rate on the cluster sizes, and $\Phi(1,1) = 1$. To describe the behaviour of the steady-state cluster-size distribution function $n_s(h,\infty)$ we generalize the scaling assumption (8.24) to reversible aggregation. In (8.24) the argument of the scaling function was equal to the ratio of the cluster size s to the mean cluster size $S(t)$ (8.15). We expect that the value of the mean cluster size in reversible CCA for $t \to \infty$ scales with the fragmentation rate as (Family *et al* 1986)

$$S(h,\infty) \sim h^{-y}. \tag{8.28}$$

The above expression combined with (8.18) and (8.24) provides the following scaling assumption

$$n_s(h,\infty) \sim s^{-2} f(sh^y) \tag{8.29}$$

for the number of clusters of size s in a unit volume in the long time limit. The scaling function $f(x)$ is expected to behave as $f(x) \sim x^{2-\tau}e^{-cx}$, where the exponent τ and the constant c depend on the actual choice for F_{ij}. The scaling assumption (8.29) implies that $n(h,\infty) \sim k^y$ for the total (normalized) number of clusters.

The scaling form (8.29) can be checked by simulations. In order to avoid the complexities originating in the geometrical properties of the clusters it is practical to use the particle coalescence model in which clusters are represented by single sites (Kang and Redner 1984). However, when two clusters of masses i and j meet they coalesce into a heavier single-site cluster of mass $i+j$. The breakup probability (8.27) is chosen to be $F_{ij} = h(i+j)^\alpha$.

According to the *simulations* of the above model (Family *et al* 1986) the exponent y determined for various α is independent of the dimension of the lattice on which the aggregation process takes place for $1 \leq d \leq 3$.

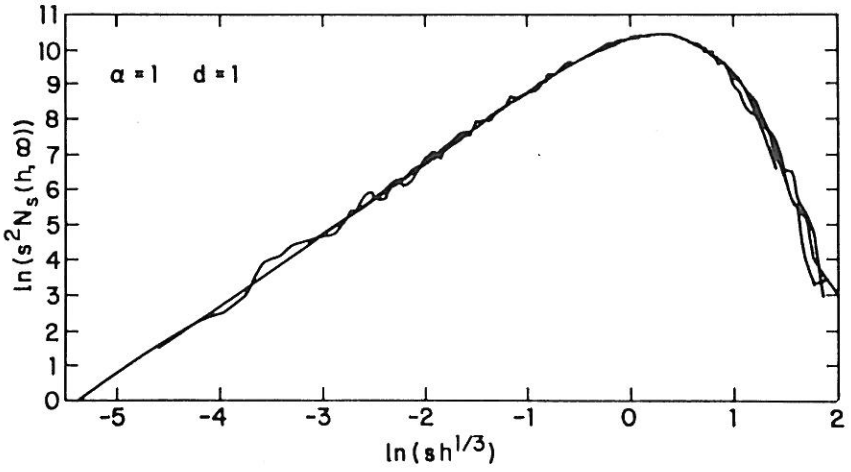

Figure 8.12. Scaling of the steady-state cluster-size distribution function $N_s(h,\infty)$ obtained from one-dimensional simulations carried out with breakup constants $k = 10^{-4}$, 10^{-5}, 10^{-6} and 10^{-7} (Family *et al* 1986).

In addition, the scaling law $y = 1/(\alpha + 2)$ resulting from the mean-field Smoluchowski equation approach (next Section) is satisfied in all cases as well. Thus we conclude that in contrast to irreversible aggregation, the spatial fluctuations in the density of the particles are compensated by the fragmentation effect down to at least one dimension, i.e., *the upper critical dimension* is $d_c \leq 1$. The agreement with the scaling assumption (8.29) for the cluster-size distribution is demonstrated in Fig. 8.12, where the one-dimensional results for the quantity $s^2 N_s(h,\infty)$ obtained for $\alpha = 1$ and various values of h are scaled into a universal function when plotted against sk^y. Similar agreements exist for $d = 2$ and $d = 3$ and for other values of α.

8.2.4. Mean-field theories

The classical understanding of aggregation kinetics is given by the *rate equation approach* proposed by Smoluchowski (1917). The basic assumptions of his theory are the following. i) The reaction rate K_{ij} for two clusters of masses i and j is about the same for any pair of clusters having masses i and j, respectively. ii) The concentration of clusters with a given mass can be represented by its spatial average. Thus the space dependence of all quantities is neglected, consequently, this approach is an intrinsically mean-field

theory. iii) Finally, it is assumed that the system is sufficiently diluted so that the reaction rate between two types of clusters is not influenced by the presence of other clusters.

With these assumptions the rate of aggregation of i-clusters with j-clusters to form a cluster of mass $i+j$ is proportional to the concentration of reactants $Rate \sim K_{ij} n_i(t) n_j(t)$, where K_{ij} is called the collision matrix or kernel. Smoluchowski's equation is then found by writing the population balance equation, taking into account both the gains and losses due to collisions

$$dn_s(t)/dt = \frac{1}{2} \sum_{i+j=s} K_{ij} n_i(t) n_j(t) - n_s(t) \sum_{j=1}^{\infty} K_{sj} n_j(t). \qquad (8.30)$$

Thus the above coagulation equation constitutes an infinite set of coupled non-linear rate equations which have to be solved for a given initial distribution $n_s(t=0)$. Eq. (8.30) has been studied extensively for decades, and there exists a vast number of papers in the literature devoted to the description of its properties. Here only those aspects of the Smoluchowski approach will be discussed which are closely related to fractal aggregation and its simulation.

The question of validity of (8.30) for *diffusion-limited CCA* arises naturally. It can be investigated by checking the collision rates and the evolution of the cluster-size distribution during the simulation of CCA and relating the results to those obtained from the Smoluchowski theory. From the point of view of Eq. (8.30) the question translates into finding the form of the collision matrix when the clusters are fractal. Smoluchowski showed that for diffusing, simple spherical clusters in $d = 3$ the coagulation kernel is proportional to $K_{i,j} \sim \left(i^{1/3} + j^{1/3}\right)\left(i^{-1/3} + j^{-1/3}\right)$, where the first term of the right-hand side is related to the effective cross-section proportional to the sum of the cluster radii $R_i + R_j$ and the second term is the sum of the diffusivities of the two colliding clusters (according to the Stokes-Einstein formula, the mobility of a cluster is inversely proportional to its radius).

Assuming that the cluster diffusivity depends on i as i^{γ} (8.1) one expects for the kernel describing diffusion-limited CCA

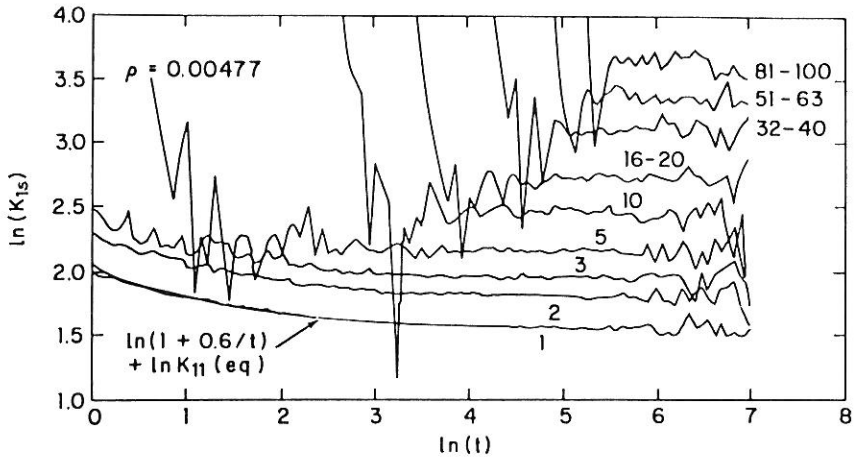

Figure 8.13. Effective collision rates K_{1s} for $\gamma = 0$ determined from simulations of diffusion-limited cluster-cluster aggregation on a simple cubic lattice (Ziff *et al* 1985).

$$K_{ij} \sim \left(i^{1/D} + j^{1/D}\right)^{d-2} \left(i^{\gamma} + j^{\gamma}\right). \tag{8.31}$$

The coefficients K_{ij} can be determined from simulations by counting the number of collisions in unit time between clusters of masses i and j and dividing this number by $n_i(t)n_j(t)$. Fig. 8.13 shows the results for the effective K_{1s} for $\gamma = 0$. The large fluctuations are due to the small number of clusters of the given size at the given stage of the aggregation process. The mean-field approximation is verified by the fact that the collision kernel is apparently independent of time except for small times (Ziff *et al* 1985).

In the most relevant physical situations the collision kernel is a homogeneous function of its variables (see e.g. Botet and Jullien 1984, Ernst 1985)

$$K_{\lambda i \lambda j} = \lambda^{2\omega} K_{ij}. \tag{8.32}$$

Obviously, (8.31) satisfies this condition with

$$2\omega = (d-2)/D + \gamma. \tag{8.33}$$

It is possible to relate ω to the dynamic exponent z describing the time development of the typical cluster size which is defined as the second moment of $n_s(t)$ (8.15). The dominant contribution to its increase arises from aggregates of comparable size. In this approximation, the sums in the rate equation are reduced to a single term involving the reaction of two clusters of half of the typical size. Calculating the second moments of the two sides of the resulting equation gives (Leyvraz 1984, Kang *et al* 1986)

$$\frac{dS(t)}{dt} \sim K_{SS} \sim [S(t)]^{2\omega}. \tag{8.34}$$

Since $S(t) \sim t^z$ (8.15), one obtains from (8.34)

$$z = \frac{1}{1-2\omega}. \tag{8.35}$$

Substituting (8.33) into (8.35) we find a relation between the dynamic exponent z, the mobility exponent γ and the fractal dimension D (Kolb 1984)

$$z = \frac{1}{1-\gamma-(d-2)/D}. \tag{8.36}$$

Note that for the Brownian kernel $\gamma = -1/D$, thus for ordinary diffusion-limited CAA in three dimensions the above expression predicts $z = 1$. For $d \geq 2$, (8.36) is in agreement with the simulation and experimental data, although the numerical values show some deviations from (8.36). For example, the simulations give $z \simeq 0.85$ in $d = 3$ for $\gamma = -1$, while $z \simeq 0.7$ from (8.36). The differences in the values provided by the simulations and the predictions of the Smoluchowski equation might be due to an extremely slow crossover to the asymptotic regime. These results are consistent with the conclusion made in the previous Section that the upper critical dimension for the kinetics of CCA is $d_c = 2$ (Kang and Redner 1984, Vicsek *et al* 1985).

Reaction-limited CCA of fractal aggregates can be studied by the Smoluchowski approach assuming that the coagulation kernel is of the form (Ball *et al* 1987)

$$K_{ij} \sim i^{2\omega} \qquad \text{if} \qquad i \simeq j \tag{8.37}$$

since the kernel is expected to be proportional to the reaction surface (the number of active sites to be able to form contacts) which was shown to scale with the cluster size (8.6). For clusters of very different masses one assumes

$$K_{ij} \sim i\, j^{2\omega-1} \qquad \text{if} \qquad i \gg j. \tag{8.38}$$

The above expression follows from a picture in which the larger cluster is imagined being made of i/j blobs of mass j. Then, for $D < d$ the smaller cluster can easily penerate the larger one and the reaction surface is additive over the accessible blobs.

The solution of the Smoluchowski equation corresponding to the above kernel is known (Ernst 1985). i) For $\omega < 1/2$ the cluster-size distribution has a bell shape. ii) If $\omega = 1/2$, $n_s(t)$ decreases as $s^{-\tau}$ with $\tau = 3/2$ up to a cutoff size. iii) For $\omega > 1/2$ the solution can be interpreted in terms of gelation and $n_s(t) \sim s^{-\tau}$ with $\tau = (3+2\omega)/2 > 2$. Note that these solutions qualitatively correspond to the numerical results ontained in the simulations of CCA (see e.g. Fig. 8.7).

There is a mechanism by which the singularity of the solution at $\omega = 1/2$ can stabilize the system through the *self-adjustment of the fractal dimension D* (Ball *et al* 1987). Let us imagine the effect of increasing ω from 1/2. According to the previous paragraph this leads to an increased τ, i.e., to a greater number of smaller clusters which are able to penetrate within the larger ones. This dominant reaction will increase the fractal dimension of the large clusters. In turn, ω will be decreased since the number of active sites is less for more compact objects. However, if ω is decreased from 1/2, $n_s(t)$ becomes nearly monodisperse. Then the clusters of nearly equal size will interpenetrate substantially less than for $\omega = 1/2$, and the resulting clusters will be more open having a smaller D leading to an increase of ω. Therefore, the system can adjust D to force ω to be equal to 1. This qualitative argument is supported by stability analysis and experimental results.

The Smoluchowski equation can be used to obtain relations among the exponents describing the scaling behaviour of *steady-state CCA*. Feeding single particles into the system can be represented by the term $k\delta_{s1}$, while the elimination of clusters containing more than s_r particles means that $n_s(t) = 0$ for $s > s_r$. With these changes (8.30) has the form

$$dn_s(t)/dt = k\delta_{s1} + 1/2 \sum_{i+j=s\leq s_r} K_{ij} n_i n_j - n_s \sum_{j=1}^{s_r} K_{js} n_j. \tag{8.39}$$

The above rate equation represents a special case of the more general equation (Rácz 1985a)

$$dn_s(t)/dt = k\delta_{s1} - G_s(n_1, n_2, ..., n_r), \tag{8.40}$$

where G_s is a homogeneous function of degree δ

$$G_s(\lambda n_1, \lambda n_2, ..., \lambda n_r) = \lambda^{1/\delta} G_s(n_1, n_2, ..., n_r) \tag{8.41}$$

with $\delta = 1/2$. The scaling analysis of (8.40) for general δ can be carried out by rescaling the time and the cluster-size distribution

$$\tilde{t} = k^{1-\delta}, \qquad \tilde{n}_s(\tilde{t}) = \frac{n_s(t)}{k^\delta}. \tag{8.42}$$

Using the above variables k is eliminated from (8.40), and this means that the solution for large t can be written in the form

$$n_s(t) = k^\delta \phi_s(k^{1-\delta} t) \tag{8.43}$$

which is exact only if $n_j(0) \sim k^{1/\delta}$. However, one expects that the steady-state properties are insensitive to the initial conditions. Accordingly, for the total number of clusters, $\sum_s n_s(t)$, one has

$$n(t) = k^\delta \phi(k^{1-\delta} t). \tag{8.44}$$

This relation is in agreement with the scaling form (8.24) suggested by the simulations with (Rácz 1985a)

$$\delta + \Delta = 1. \tag{8.45}$$

Since for zero feeding rate $n(t) \sim t^{-z}$ (8.16), $\phi(x)$ must behave for $x \ll 1$ as x^{-z} and from (8.44) we obtain another scaling law

$$\delta = z\delta. \tag{8.46}$$

For the original Smoluchowski equation $\delta = \Delta = 1/2$ and $z = 1$.

Finally, we shall use the rate equation approach to obtain a relation among the exponents describing *reversible CCA*. In the stationary limit the left-hand side of the Smoluchowski equation (8.30) vanishes, and with the breakups taken into account it can be written as

$$0 = \frac{1}{2}\sum_{i+j=s}[K_{ij}n_in_j - F_{ij}n_{i+j}] - \sum_{j=1}^{\infty}[K_{sj}n_sn_j - F_{sj}n_{s+j}], \tag{8.47}$$

where F_{ij}, the breakup rate (8.27), is assumed to have the scaling property

$$F_{\lambda i\lambda j} = \lambda^{\alpha}F_{ij}. \tag{8.48}$$

This type of scaling is satisfied by most of the physically relevant forms of F_{ij}. To obtain an expression for the exponent y defined by (8.28), we also assume that the rate equation (8.47) is invariant under the scaling transformation $h \to \lambda h$ and $s \to \lambda^y s$. Then using (8.29), (8.32) and (8.48) in (8.47) one gets (Family *et al* 1986)

$$y = \frac{1}{\alpha - 2\omega + 2}. \tag{8.49}$$

This relation is supported by explicit results for fragmentation models satisfying detailed balance (Ernst and van Dongen 1987) and by numerical sim-

ulations (Section 8.2.3.) of the particle coalescence model in which $y \simeq 0.66$ was obtained for $\omega = 0$ and $\alpha = -1/2$.

8.3. EXPERIMENTS ON CLUSTER-CLUSTER AGGREGATION

The aggregation of clusters of particles can take place in a wide variety of experimental conditions. For example, the first quantitative analysis of the fractal nature of cluster-cluster aggregates was carried out for clusters of metallic smoke particles formed in air. If the particles interact through an attractive force and the aggregates are mobile, the resulting structures normally have fractal properties. The key point is that the bond which is formed between two particles has to be more or less *rigid*. Otherwise, surface diffusion and evaporation lead to considerable restructuring of the aggregates terminating in simple shapes characteristic for equilibrium morphologies. In most of the cases the relative stiffness of bonds is provided by the size of the aggregating particles: atoms or small molecules are usually mobile on the surface of a growing object, while microscopic particles consisting of a large number of atoms tend to stick to each other rigidly. Colloidal suspensions of metallic or other particles are the most typical systems of this kind. Polymer molecules can also form stiff bonds.

Two approaching particles do not stick necessarily, even if there exists a short range attractive force between them, because a repulsive barrier, V_r, in the interaction potential may prevent the particles from forming a bond. The probability of sticking is proportional to $p_s \sim \exp(-V_r/k_BT)$, and depending on the value of V_r, the aggregation is *diffusion-limited* ($p_s \simeq 1$) or *reaction-limited* ($p_s \ll 1$). A common source for the repulsion term is the electric charge accumulated on the surface of the particles. This charge can be compensated by adding appropriate substances, and the diffusion and reaction-limited regimes can be studied in the same colloidal system.

8.3.1. Structure

Gold colloids are particularly suitable for studying Brownian clustering phenomena. This was recognized by Faraday who studied their stability and resistance to aggregation. The main advantages of using gold colloids are the following (Weitz and Oliviera 1984a, 1984b). i) The freshly made suspension typically consists of highly uniform spherical particles with a size distribution characterized by a root-mean-square deviation of about 10%. ii) the particles stick irreversibly since gold metal bonding is likely to occur at the point two spheres touch. iii) the rate of aggregation can easily be controlled by adding pyridine to the system. Finally, iv) the structure of gold particles can be examined by transmission electron-microscope (TEM) techniques, because they give images with high contrast and do not suffer from charging problems when using an electron beam.

The standard recipe to make gold colloids is the reduction of a gold salt $Na(AuCl_4)$ with sodium citrate. In a typical experiment the mean diameter of particles is about 15 nm, and they are separated at the beginning by about 60 particle diameters corresponding to a volume fraction of $\sim 10^{-6}$. The diffusion constant associated with the particles is approximately $5 \times 10^{-7}\text{cm}^2/\text{sec}$, which results in a diffusion time $\sim$ 10msec on a length scale of the interparticle distance.

In the course of their formation the gold spheres become covered by citrate ions, creating a large negative surface charge. The ions in the solution produce a Debye-Hückel screening length of the same order as the particle diameter. The resulting short range repulsive interaction makes the colloids rather stable against aggregation. However, it is possible to eliminate the negative charge on the surface of the particles by adding neutral pyridine molecules to the solution which being absorbed on the surface of the gold spheres displace the negative citric ions. As a result aggregation times ranging from several minutes (fast or diffusion-limited CCA) to several weeks (slow or reaction-limited CCA) can be realized.

The real space visualization of *three-dimensional gold colloid* aggregates is achieved by preparing TEM grids using samples of the solution at

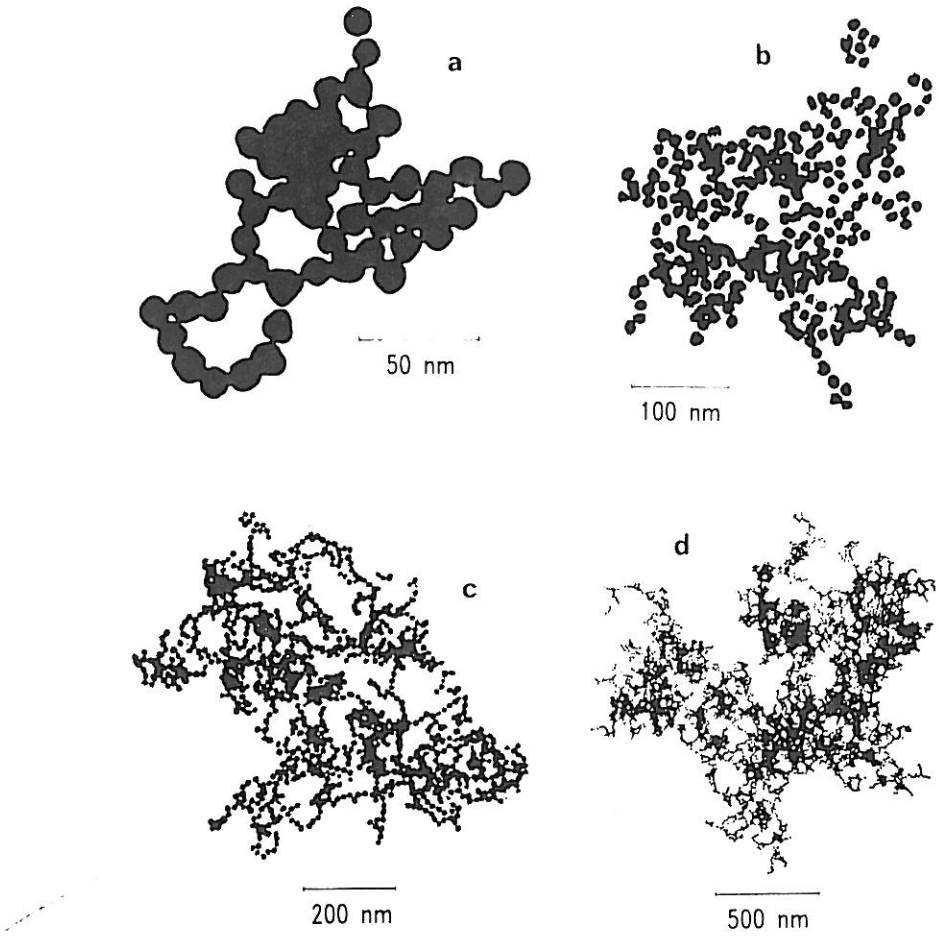

Figure 8.14. Transmission electron micrographs of gold colloid aggregates. These projected images correspond to three-dimensional clusters of various sizes. The largest aggregate consists of 4739 spherical gold particles (Weitz and Oliviera 1984b).

several points in time (Weitz and Oliviera 1984). The TEM grids consist of an approximately 20nm thick carbon film supported by a copper grid. As the fluid evaporates the surface tension pulls the aggregates straight down to the grid, i.e., "flattens" them causing only a small distortion of the true geometric *projection*. Therefore, in this approach it is the two-dimensional projection of the three-dimensional clusters which is used to obtain information about the structure. According to rule a) in Section 2.2., the fractal dimension of an object projected onto a plane is equal to that of the original one if $D < 2$. In the case $D > 2$, the projected structure does not exhibit scale invariance.

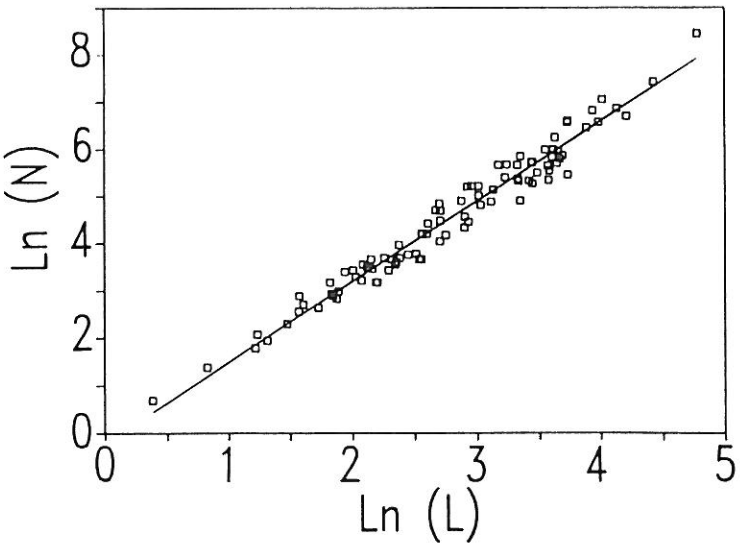

Figure 8.15. Determination of the fractal dimension of gold colloid aggregates by plotting the number of particles in the clusters versus their linear size L. The slope gives $D \simeq 1.75$ (Weitz and Oliviera 1984a).

During *fast* aggregation the particles stick at the first time they collide. Fig. 8.14 shows representative pictures of aggregates taken from a single grid. Although these pictures are two-dimensional projections, they have open, ramified geometry and the number of areas corresponding to overlapping particles is relatively small. Thus we can assume that the aggregates are fractals with a dimension smaller than 2. In fact, the scale invariance of the structure of aggregates is nicely demonstrated by the fact that the properly magnified small clusters have an overall appearance similar to the shape of the largest aggregate. In order to obtain an estimate for the fractal dimension of the aggregates, one can measure the number of particles N in a cluster as a function of the linear size L. For a fractal of dimension D one expects $N \sim L^D$ (2.2). In Fig. 8.15 $\ln N$ is plotted against $\ln L$, and the straight line giving the best fit to the data indicates that the structure of gold colloid aggregates is characterized by a fractal dimension $D \simeq 1.75$ in good agreement with the computer simulations of diffusion-limited CCA yielding essentially the same value.

During reaction-limited or *slow* aggregation the particles form a bond

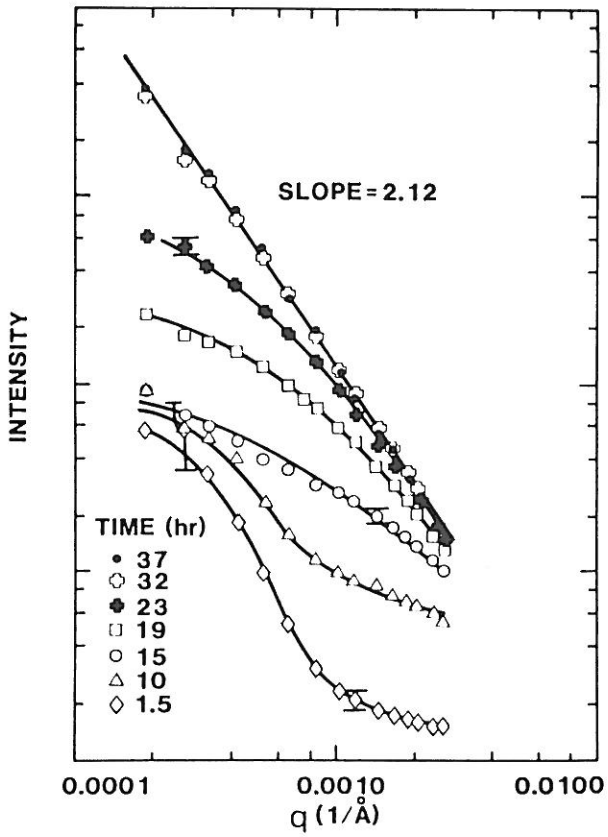

Figure 8.16. Scattered light intensity profiles for various times. The growth of fractal silica aggregates is indicated by the uppermost series of data coresponding to a fractal dimension of $D \simeq 2.12$ (Schaefer *et al* 1984).

with a small probability (they collide many times before sticking). In addition to gold colloids (Weitz *et al* 1985), this limit can be investigated using silica particles of diameter $\simeq 27$ Å(Schaefer *et al* 1984). Again, the surface charge has to be reduced to provide a sticking probability larger than 0, but much less than 1. This can be accomplished by reducing the *p*H to 5.5 in the solution contaning silica monomers, while increasing the salt concentration to ≥ 0.5 M.

To analyse the structure of the growing silica aggregates (Schaefer *et al* 1984) one can also use light scattering and small angle x-ray scattering (SAXS), as an alternative to transmission electron microscopy. In Section 4.1. it has been shown that scattered intensity from a fractal of dimension D scales with the wave number of the radiation, q, as $I(q) \sim q^{-D}$. This re-

lation is valid for wave numbers corresponding to linear sizes larger than the diameter of the particles and smaller than the linear size of the aggregates. Obviously, it can be applied to an ensemble of clusters as well, if the size distribution of aggregates is approximately monodisperse (for diffusion-limited dynamics this condition is usually satisfied). Even if the cluster-size distribution is not monodisperse, the scattered intensity at any q is dominated by the contributions from the largest clusters if $\tau < 2$, a condition which is satisfied as well (see Section 8.2.1). An important advantage of the scattering techniques is that they allow *in situ* measurement of the geometrical properties, i.e., there is no need for sample preparation before the application of the method.

Fig. 8.16 shows the temporal development of the scattered light intensity. The non-trivial time dependence of the data is explained by the observation that after a relatively short time a few large clusters were visible through a telescope in the scattering volume. These clusters are responsible for the relatively quick increase of the intensity for small q. The error bars decrease as the aggregation proceeds, and the maximum grows two decades in intensity until 37 h after initiation. $I(q)$ behaves as a power law in the range 5000Å$> q^{-1} >$500Å. The slope on this log-log plot corresponds to a fractal dimension $D \simeq 2.1$ which agrees well with the simulation results (for the polydisperse case the reaction-limited CCA model gives $D \simeq 2.1$ as well). The combination of light scattering with SAXS makes it possible to demonstrate that the fractal scaling extends over two decades.

Due to the gravitational force large aggregates growing in three dimensions leave the active volume of the system because of sedimentation. This problem does not arise in *two-dimensional* systems. Carrying out experiments on $2d$ CCA has additional advantages. i) It makes the visualization of the results much easier. This is illustrated by Fig. 8.17, where ordinary photographs taken from aggregates of carbon particles floating on water are shown (Horkai and Bán 1988). ii) Two-dimensional aggregation takes place on surfaces and such processes are interesting from a practical point of view as well. iii) Changing the properties of the interface the aggregation process can be controlled. Finally, the high density limit of CCA can be realized and

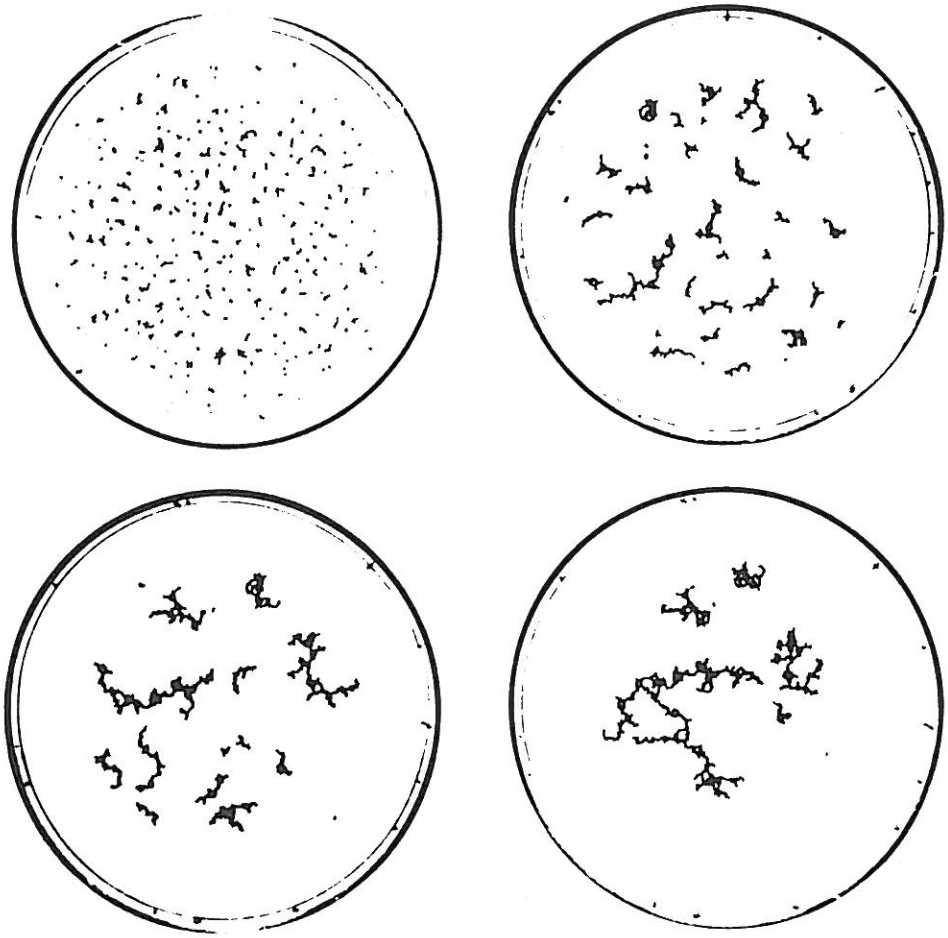

Figure 8.17. Snapshots of carbon particle aggregates illustrating two-dimensional CCA. Since the diameter of the particles used in this experiment was relatively large (approximately 0.5mm), surface tension effects dominated the process and the clusters moved along essentially straight lines rather than Brownian trajectories (Horkai and Bán 1988).

studied easier.

One of the common ways to study diffusion-limited cluster-cluster aggregation on a surface is to use a fluid–air interface where the charged colloidal particles are trapped by surface tension. For example, a fresh suspension of silica micropheres of diameter 3000Å can be dispensed onto the flat surface of water with the simultaneous injection of a methanol spreading agent. In this experiment the electrostatic repulsion of particles is screened by adding salt (1.0N CaCl) to the water. The aggregation process can be followed by optical observations and making photomicrographs. The ob-

tained pictures are suitable for digital image processing, and the methods discussed in Section 4.2. can provide estimates for the fractal dimension of the aggregates.

From the log-log plot of the radius of gyration versus the number of particles in the individual aggregates the estimate 1.20 ± 0.15 was obtained for the fractal dimension of the silica clusters (Hurd and Schaefer 1985). This value is considerably smaller than $D \simeq 1.43$ which was calculated for computer simulated cluster-cluster aggregates. The discrepancy can be interpreted using the Debye-Hückel theory for the calculation of the electric field in the vicinity of a small aggregate. The estimates for a particle approaching a dimer show that the barrier for end-on approach is much lower than for particles trying to stick to the side. Thus, a growing cluster has a tendency not to branch when there are repulsive forces present. This effect is expected to decrease the fractal dimension, at least for sizes below the asymptotic limit. An analogous decrease in D was observed in the simulations of chain-chain CCA, where side-branching is entirely prohibited.

The complexity of the situation is illustrated by the fact that there are two more fractal dimension values which can be observed in two-dimensional CCA. Aggregation of polystyrene spheres of diameter 4.7μm confined between two glass plates led to fractal structures with $D \simeq 1.49$ (Skjeltorp 1987). In this system two touching clusters are likely to rotate around the point of contact until at least three particles touch simultaneously. This rearrangment seems to eliminate the above discussed anisotropy of sticking probability and the result is in a better agreement with $D \simeq 1.48$ obtained from the simulations of the corresponding CCA model. Finally, a fractal dimension $D \simeq 1.7$ was observed in the experiments on the two-dimensional aggregation of polyvynil toluene (Armstrong *et al* 1986). To interpret this value we recall that investigations of the diffusion-limited CCA model with relatively high densities showed that structures with a fractal dimension about 1.7 are formed in the system close to its gelation point, i.e., when a cluster spanning the whole cell is formed.

8.3.2. Dynamics

Some of the predictions of the dynamic scaling theory for the cluster-size distribution, n_s, described in Section 8.2.1. can be checked by carrying out quasielastic light scattering experiments (Weitz *et al* 1984, Feder *et al* 1984). Such measurements are made while the aggregation goes on, thus the time dependence of the growth process can be conveniently monitored. According to the standard theory of dynamic light scattering (Berne and Pecoria 1976) the first cumulant of the autocorelation function of the scattered light is given by

$$K_1 = \frac{1}{I(q,0)} \int s^2 n_s(t) S_s(q)(D_s q^2 + A) ds, \tag{8.50}$$

where q is the scattering vector, D_s and A are respectively the translational and rotational diffusion constants of clusters of mass s, and $I(q,0)$ is the time averaged total scattered intensity. The structure factor of an s-cluster depends on the fractal dimension D in the form $S_s(q) \sim s^{-1} q^{-D}$ (see Section 4.1.). For fractal aggregates the dominant contribution to the decay of the intensity autocorrelation function comes from the translational term in which the cluster diffusivity can be estimated as $D_s \sim R_s^{-1} \sim s^{-1/D}$, where R_s is the radius of a cluster consisting of s particles. In this approximation the first cumulant becomes a moment of the cluster-size distribution function

$$K_1 \sim \int s^{1-1/D} n_s(t) ds. \tag{8.51}$$

The analysis of similar expressions in Section 8.2.1. showed that for $\tau < 2 - 1/D$ the above integral gives an estimate for $R^{-1}(t) \sim S^{-1/D}(t) \sim t^{-z/D}$, where $R(t)$ is the average cluster radius at time t and $S(t)$ denotes the mean cluster size. Here the exponents τ and z describe the static and dynamic scaling of the cluster-size distribution which scales as $n_s \sim s^{-\tau}$ up to a cutoff at sizes proportional to t^z. For diffusion-limited CCA in $d = 3$ it was also shown that $z \simeq 1$, therefore, we expect

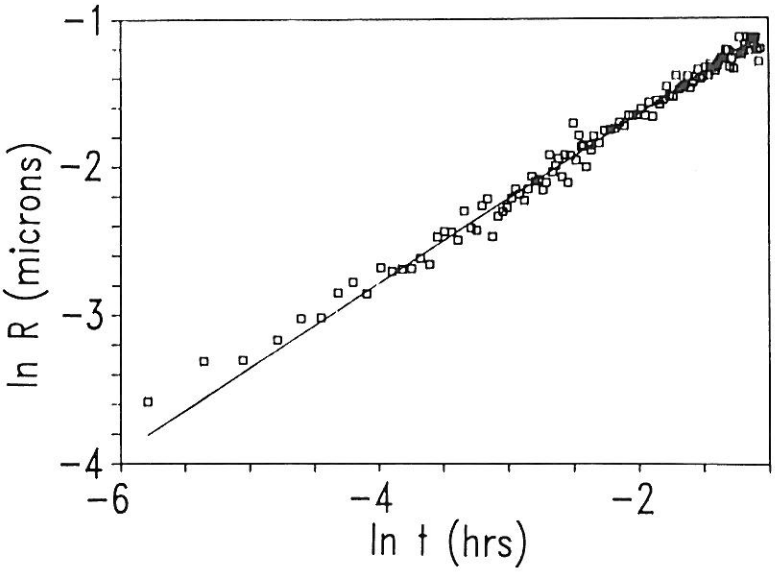

Figure 8.18. Scaling of the mean cluster radius of gold colloid aggregates with time. The slope indicates a fractal dimension $1/0.56 \simeq 1.79$ (Weitz *et al* 1984).

$$(K_1)^{-1} \sim R(t) \sim t^{1/D}. \tag{8.52}$$

Gold colloids represent suitable systems for studying aggregation kinetics as well (Weitz *et al* 1984). In Fig.8.18, $\ln R(t)$ determined from measuring K_1 for gold colloids is plotted versus the time variable t. The straight line fitted to the data has a slope of 0.56 which corresponds to a fractal dimension $D \simeq 1.79$ being close to the value obtained from simulations and independent experiments. The agreement supports the dynamic scaling assumption (8.18) for $n_s(t)$.

For reaction-limited aggregation the dynamics of growth is qualitatively different (Weitz *et al* 1985). Instead of scaling with time according to an exponent that is less than 1, the behaviour of the mean radius is better described by an exponential increase $R \sim e^{Ct}$, where C depends on the experimental conditions. If the repulsion between the gold particles is partially compensated, the dynamics is initially exponential (slow) which crosses over to exhibit the behaviour characteristic for diffusion-limited aggregation. These regimes are demonstrated in Fig 8.19. The initially exponential in-

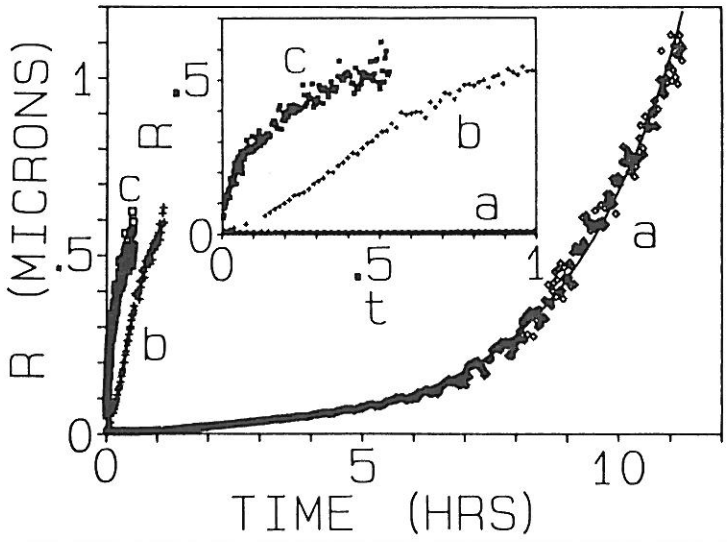

Figure 8.19. Increase of the characteristic cluster size during the aggregation of gold particles. Three kinds of kinetics can be observed: (curve a) reaction-limited, (curve b) crossover, and (curve c) diffusion-limited. The inset shows the initial behaviour on an expanded scale. The reaction-limited kinetics can be well approximated with an exponential (Weitz *et al* 1985).

crease of $R(t)$ and its subsequent crossover to a power law growth is consistent with the simulation results shown in Fig 8.9, where the total number of clusters $N(t)$ is plotted for a small constant sticking probability. For $\tau < 1$ one has $R(t) \sim [N(t)]^{-1/D}$ and indeed, $N(t)$ in Fig. 8.9 behaves as expected from this relation and Fig. 8.19.

A direct test of the dynamic scaling for $n_s(t)$ can be carried out by analysing TEM images of the clusters of gold particles on TEM grids prepared at several times during the aggregation process (Weitz and Lin 1986). The number of particles in the aggregates is counted, and the data are compiled in histograms. Two kinds of plots have been obtained: i) $n_s(t)$ exhibits a reasonably well-defined peak as a function of s for diffusion-limited CCA, while ii) it decays as a power law for reaction-limited aggregation. In addition, the cluster-size distributions can be scaled onto a single curve in both cases, which indicates dynamic scaling of the form (8.18).

Dynamic scaling can also be observed in other aggregating systems.

For example, in dilute solutions of polyfunctional monomer molecules, an ensemble of branched polymers is formed as smaller molecules are linked through new chemical bonds. A standard technique to monitor the process of polymerization is infrared spectroscopy which gives the number of bonds in the system, instead of the number of monomers. Because of this property of the method the formalism elaborated in 8.2.1. has to be modified (Djordjevic *et al* 1986). To account for the fact that only the bonds are detected experimentally, the system should be characterized by $n_b(t)$, which is the number of clusters with b chemical bonds in them. Since the total number of bonds is not a conserved quantity (it grows permanently), the scaling form for

$$n_b(t) \sim b^{-\theta} f(b/t^z) \tag{8.53}$$

is expected to hold with $\theta = 1.5$ instead of $\theta = 2$, where the latter relation was shown (Section 8.2.1) to be a consequence of mass conservation.

REFERENCES (PART II)

Aharony, A., 1985 in *Scaling Phenomena in Disordered Systems* edited by R. Pynn and A. Skjeltorp (Plenum Press, New York) p. 289

Alexander, S. and Orbach, R., 1982 *J. Physique Lett.* **43**, 2625

Alexandrowitz, Z., 1980 *Phys. Lett.* **80A**, 284

Amit, D. J., Parisi, G. and Peliti, L., 1983 *Phys. Rev.* **B27**, 1635

Amitrano, C., Coniglio, A. and di Liberto, F., 1986 *Phys. Rev. Lett.* **57**, 1016

Armstrong, A. J., Mocklet, R. C. and O'Sullivan, W. J., 1986 *J. Phys.* **A19**, L123

Balberg, I., 1988 *Phys. Rev.* **B37**, 2391

Ball, R. C. and Witten, T. A., 1984a *Phys. Rev.* **A29**, 2966

Ball, R. C. and Witten, T. A., 1984b *J. Stat. Phys.* **36**, 873

Ball, R. C., Brady, R. M., Rossi, G. and Thompson, B. R., 1985 *Phys. Rev.*

Lett. **55**, 1406

Ball, R. C., 1986 *Physica* **140A**, 62

Ball, R. C., Weitz, D. A., Witten, T. A. and Leyvraz, F., 1987 *Phys. Rev. Lett.* **58**, 274

Bansil, R., Herrmann, H. J. and Stauffer, D., 1985 *Macromolecules* **17**, 998

Barrow, J. D., 1981 *J. Phys.* **A14**, 729

Berne, B. J., and Pecora, R., 1976 *Dynamic Light Scattering* (Wiley, New York)

Binder, K., 1967 *Ann. Phys. (N.Y.)* **98**, 390

Botet, R., Jullien, R. and Kolb, M., 1984 *J. Phys.* **A17**, L75

Botet, R. and Jullien, R., 1984 *J. Phys.* **A17**, 2517

Botet, R. and Jullien, R., 1985 *Phys. Rev. Lett.* **55**, 1943

Brown, W. D. and Ball, R. C., 1985 *J. Phys.* **A18**, L517

Bunde, A., Herrmann, H., J., Margolina, A. and Stanley, H. E., 1985a *Phys. Rev. Lett.* **55**, 653

Bunde, A., Herrmann, H. J. and Stanley, H. E., 1985b *J. Phys.* **A18**, L523

Cardy, J. L. and Grassberger, P., 1985 *J. Phys.* **A18**, L267

Chandler, R., Koplik, J., Lerman, K. and Willemsen, J., 1982 *J. Fluid Mech.* **119**, 249

Chhabra, A., Matthews-Morgan, D., Landau, D. P. and Herrmann, H. J., 1984 in *Kinetics of Aggregation and Gelation* edited by F. Family and D. P. Landau (North-Holland, Amsterdam)

Chhabra, A., Landau, D. P. and Herrmann, H. J., 1986 in *Fractals in Physics* edited by L. Pietronero and E. Tossati (North-Holland, Amsterdam)

Dhar, D., 1985 in *On Growth and Form* edited by H. E. Stanley and N. Ostrowsky (Martinus Nijhoff, Dordrecht) p. 288

Debierre, J. M. and Turban, L., 1986 *J. Phys.* **A19**, L131

Debierre, J. M. and Turban, L., 1987 *J. Phys.* **A20**, L259

Djordjevic, Z. B., Djordjevic, Z. V. and Djordjevic, M. B., 1986 *Phys. Rev.* **A33**, 3614

Eden, M., 1961 in *Proc. 4-th Berkeley Symp. on Math. Statistics and Probability*, Vol. 4., Ed. F. Neyman (Berkeley, University of California Press)

Edwards, S. F. and Wilkinson, D. R., 1982 *Proc. Royal Soc. London* **A381**,

17

Ernst, M. H., 1985 in *Fundamental Problems in Statistical Mechanics VI* edited by E. G. D. Cohen (Elsevier, Amsterdam) p. 329

Ernst, M. H. and van Dongen, P. G. J., 1987 *Phys. Rev.* **A36**, 435

Family, F., Vicsek, T. and Meakin, P., 1985 *Phys. Rev. Lett.* **55**, 641

Family, F. and Vicsek, T., 1985 *J. Phys.* **A18**, 75

Family, F., Meakin, P. and Vicsek, T., 1985 *J. Chem. Phys.* **83**, 4144

Family, F., 1986 *J. Phys.* **A19**, L441

Family, F. and Hentschel, 1987 *Faraday Discuss. Chem. Soc.* **83** paper 6

Family, F., Meakin, P. and Deutch, J. M., 1986 *Phys. Rev. Lett.* **57**, 727

Family, F., Platt, D. and Vicsek, T., 1987 *J. Phys.* **A20**, L1177

Feder, J., Jossang, T. and Rosenquist, E., 1984 *Phys. Rev. Lett.* **53**, 1403

Fisher, M. E., 1967 *Rep. Prog. Phys.* **30**, 615

Flory, P., 1971 *Principles of Polymer Chemistry* (Cornell Univ. Press, Ithaca)

Forrest, S. R. and Witten, T. A., 1979 *J. Phys.* **A12**, L109

Freche, P., Stauffer, D. and Stanley, H. E., 1985 *J. Phys.* **A18**, L1163

Friedlander, S. K., 1977 *Smoke, Dust and Haze: Fundamentals of Aerosol Behaviour* (Wiley, New York)

Garik, P., Richter, R., Hautman, J. and Ramanlal, P., 1985 *Phys. Rev.* **A32**, 3156

Gefen, Y., and Aharony, A. and Alexander, S., 1983 *Phys. Rev. Lett.* **50**, 77

de Gennes, P. G., 1979 *Scaling Concepts in Polymer Physics* (Cornell Univ. Press, Ithaca)

Gould, H., Family, F. and Stanley, H. E., 1983 *Phys. Rev. Lett.* **50**, 686

Grassberger, P., 1983 *Math. Biosci.* **62**, 157

Grassberger, P., 1985 *J. Phys.* **A18**, L215

Guyer, R. A., 1984 *Phys. Rev.* **A30**, 1112

Halsey, T. C. and Meakin, P., 1985 *Phys. Rev.* **A32**, 2546

Halsey, T. C., Meakin, P. and Procaccia I., 1986 *Phys. Rev. Lett.* **56**, 854

Halsey, T. C., 1987 *Phys. Rev. Lett.* **59**, 2067

Havlin, S. and Ben-Avraham, D., 1987 *Advances in Physics* **36**, 695

Hayakawa, Y., Sato, S. and Matsushita, M., 1987 *Phys. Rev.* **A36**, 1963

Herrmann, H. J., Landau, D. P. and Stauffer, D., 1982 *Phys. Rev. Lett.* **49**, 412

Herrmann, H. J. and Stanley, H. E., 1984 *Phys. Rev. Lett.* **53**, 1121

Herrmann, H. J. and Stanley, H. E., 1985 Z. Physik **60**, 165

Herrmann, H. J., 1986 *Phys. Rep.* **36**, 153

Honda, K., Toyoki, H. and Matsushita, M., 1986 *J. Phys. Soc. Jpn.* **55**, 707

Horkai, F. and Bán, S., 1988 unpublished

Hurd, A. J., and Schaefer, D. W., 1985 *Phys. Rev. Lett.* **54**, 1043

Joag, P. S., Limaye, A. V. and Amritkar R. E., 1987 *Phys. Rev.* **A36**, 3395

Jullien, R. and Botet, R., 1985 *J. Phys.* **A18**, 2279

Jullien, R. and Kolb, M., 1984 *J. Phys.* **17**, L639

Jullien, R. and Meakin, P., 1987 *Europhys. Lett.* **4**, 1385

Jullien, R., 1984 *J. Phys.* **A17**, L771

Kang, K. and Redner, S., 1984 *Phys. Rev.* **A30**, 2833

Kang, K., Redner, S., Meakin, P. and Leyvraz, F., 1986 *Phys. Rev.* **A33**, 1171

Kapitulnik, A., Aharony, A., Deutscher, G. and Stauffer, D., 1983 *J. Phys.* **A16**, L269

Kardar, M., Parisi, G. and Zhang, Y. C., 1986 Phys. Rev. Lett **56**, 889

Kardar, M. and Zhang, Y. C., 1987 *Phys. Rev. Lett.* **58**, 2087

Kerstein, A. R. and Bug, A. L., 1984 unpublished

Kertész J. and Wolf, D. E., 1988 *J. Phys.* **A21**, 747

Kolb, M., Botet, R. and Jullien, R., 1983 *Phys. Rev. Lett.* **51**, 1123

Kolb, M., 1984 *Phys. Rev. Lett.* **53**, 1653

Kolb, M., 1985 *J. Physique Lett.* **46**, 631

Kolb, M. and Herrmann, H. J., 1987 *Phys. Rev. Lett.* **59**, 454

Kremer, K. and Lyklema, J. W., 1985a *Phys. Rev. Lett.* **55**, 2091

Kremer, K. and Lyklema, J. W., 1985b *Phys. Rev. Lett.* **54**, 267

Krug, J., 1987 *Phys. Rev.* **A36**, 5465

Leamy, H. J., Gilmer, G. M. and Dirks, A. G., 1980 in *Current Topics in Mat. Sci.* **6**, (North-Holland, Amsterdam) p. 309

Leath, P. L., 1976 *Phys. Rev.* **B14**, 5046

Lenormand, R. and Bories, S., 1980 *C. R. Acad. Sci. (Paris)* **291**, 279

Leyvraz, F., 1984 *Phys. Rev.* **A29**, 854

Leyvraz, F., 1985 *J. Phys.* **A18**, L941

Liang, S. and Kadanoff, L. P., 1985 *Phys. Rev.* **A31**, 2628

Lyklema, J. W. and Kremer, K., 1984 *J. Phys.* **A17**, L691

Lyklema, J. W., 1985 *J. Phys.* **A18**, L617

Lyklema, J. W. and Evertsz, C., 1986 in *Fractals in Physics* edited by L. Pietronero and E. Tossati (North-Holland, Amsterdam) p. 87

Madelaine, G. J., Perrin, M. L. and Itox, M., 1979 *J. Aerosol Sci.* **12**, 202

Majid, I., Jan, N., Coniglio, A. and Stanley, H. E., 1984 *Phys. Rev. Lett.* **52**, 1257

Makarov, N. G., 1985 *Proc. London Math. Soc.* **51**, 369

Manneville, P. and de Seze, L., 1981 in *Numerical Methods in the Study of Critical Phenomena* edited by I. Della Dora, J. Demongeot and B. Lacolle (Springer, New York)

Matsushita, M., Honda, K., Toyoki, H., Hayakawa, Y. and Kondo, H., 1986 **55**, 2618

McKane, A. J. and Moore, M. A., 1988 *Phys. Rev. Lett.* **60**, 527

McMurry, P. H., *J. Colloid Interface Sci.* **78**, 513

Meakin, P., 1983a *Phys. Rev.* **A26**, 1495

Meakin, P., 1983b *Phys. Rev.* **A27**, 2616

Meakin, P., 1983c *Phys. Rev. Lett.* **51**, 1119

Meakin, P., 1984 *Phys. Rev.* **B30**, 4207

Meakin, P., 1985a *J. Phys.* **A18**, L661

Meakin, P., 1985b *J. Colloid Interface Sci.* **105**, 240

Meakin, P., 1985c in *On Growth and Form* edited by H. E. Stanley and N. Ostrowsky (Martinus Nijhoff, Dordrecht) p. 111

Meakin, P. and Vicsek, T., 1985 *Phys. Rev.* **A32**, 685

Meakin, P., Leyvraz, F. and Stanley, H. E., 1985a *Phys. Rev.* **A31**, 1195

Meakin, P., Vicsek, T. and Family, F., 1985b *Phys. Rev.* **B31**, 564

Meakin, P., Coniglio, A., Stanley, H. E. and Witten, T. A., 1986a *Phys. Rev.* **A34**, 3325

Meakin, P., Ramanlal, P., Sander, L. M. and Ball, R.C., 1986b *Phys. Rev.* **A34**, 5091

Meakin, P., Ball, R. C., Ramanlal, P. and Sander, L. M., 1987 *Phys. Rev.* **A35**, 5233

Meakin, P. and Vicsek, T., 1987 J. Phys. **A20** L171

Meakin, P., 1987a *Phys. Rev.* **A35**, 2234

Meakin, P., 1987b in *Phase Transitions and Critical Phenomena* Vol. 12 edited by C. Domb and J. L. Lebowitz (Academic Press, New York)

Meakin, P. and Havlin, S., 1987 *Phys. Rev.* **A36**, 4428

Meakin, P. and Jullien, R., 1987 *J. Physique* **48**, 1651

Meakin, P., Kertész, J. and Vicsek, T., 1988 *J. Phys.* **A21**, 1271

Medalia, A. I., 1967 *J. Colloid Interface Sci.* **24**, 393

Miyazima, S., Meakin, P. and Family, F., 1987 *Phys. Rev.* **A36**, 1421

Montag, J. L., Family, F., Vicsek, T. and Nakanishi, H., 1985 *Phys. Rev.* **A32**, 2557

Muthukumar, M., 1983 *Phys. Rev. Lett.* **50**, 839

Niemeyer, L., Pietronero, L. and Wiesmann, H. J., 1984 *Phys. Rev. Lett.* **52**, 1033

Nieuwenheuzen, J. M. and Haanstra, H. B., 1966 *Philips Techn. Rev.* **27**, 87

Obukhov, S. P. and Peliti, L., 1983 *J. Phys.* **A16** L147

Ohtsuki T. and Keyes, T., 1985 *Phys. Rev.* **A33**, 1223

O'Shaughnessy, B. and Procaccia, I., 1985 *Phys. Rev. Lett.* **54**, 455

Pandey, R. B. and Stauffer, D., 1983 *Phys. Lett.* **95A**, 511

Pietronero, L., 1983 *Phys. Rev.* **B27**, 5887

Plischke, M. and Rácz, Z., 1984 *Phys. Rev. Lett.* **53**, 415

Rácz, Z. and Vicsek, T., 1983 *Phys. Rev. Lett.* **51**, 2382

Rácz, Z., 1985a *Phys. Rev.* **A32**, 1129

Rácz, Z., 1985b *Phys. Rev. Lett.* **55**, 1707

Ramanlal, P. and Sander, L. M., 1985 *Phys. Rev. Lett.* **54**, 1828

Rammal, R. and Toulouse, G., 1983 *J. Physique Lett.* **44**, 13

Rikvold, P. A., 1982 *Phys. Rev.* **A26**, 647

Rudnick, J. and Gaspari, G., 1986 *J. Phys.* **A19**, L191

Saleur, H. and Duplantier, B., 1987 *Phys. Rev. Lett.* **58**, 2325

Sapoval, B., Rosso, M. and Gouyet, J. F., 1985 *J. Physique Lett.* **46**, 149

Schaefer, D. W., Martin, J. E., Wiltzius, P. and Cannel, D. S., 1984 *Phys. Rev. Lett.* **52**, 2371

Skjeltorp, A. T., 1987 *Phys. Rev. Lett.* **58**, 1444

von Smoluchowski, M., 1917 *Z. Phys. Chem.* **92**, 129

Solc, K, 1973 *Macromolecules* **6**, 378

Stauffer, D., 1985 *Introduction to Percolation Theory* (Taylor and Francis,

London)

Sutherland, D. N., 1966 *J. Colloid Interface Sci.* **22**, 300

Sutherland, D. N., 1967 *J. Colloid Interface Sci.* **25**, 373

Tokuyama, M. and Kawasaki, K., 1984 *Phys. Lett.* **100A**, 337

Turkevich, L. A. and Scher, H., 1985 *Phys. Rev. Lett.* **55**, 1026

Turkevich, L. A. and Scher, H., 1986 *Phys. Rev.* **A33**, 786

Vicsek, T., 1983 *J. Phys.* **A16**, L647

Vicsek, T. and Family, F., 1984a *Phys. Rev. Lett.* **52**, 1669

Vicsek, T. and Family, F., 1984b in *Kinetics of Aggregation and Gelation* edited by F. Family and D. P. Landau (North-Holland, Amsterdam) p. 110

Vicsek, T., Meakin, P. and Family, F., 1985 *Phys. Rev.* **A32**, 1122

Vicsek, T., Family, F., Kertész, J. and Platt, D., 1986 *Europhys. Lett.* **2**, 823

Vold, M. J., 1963 *J. Colloid Interface Sci.* **18**, 684

Weinrib, A. and Trugman, S. A., 1985 *Phys. Rev.* **B31**, 2993

Weitz, D. A. and Oliveria, M., 1984a *Phys. Rev. Lett.* **52**, 1433

Weitz, D. A. and Oliveria, M., 1984b in *Kinetics of Aggregation and Gelation* edited by F. Family and D. P. Landau (North-Holland, Amsterdam)

Weitz, D. A., Huang, J. S., Lin, M. Y. and Sung, J., 1984 *Phys. Rev. Lett.* **53**, 1657

Weitz, D. A., Huang, J. S., Lin, M. Y. and Sung, J., 1985 *Phys. Rev. Lett.* **54**, 1416

Weitz, D. A. and Lin, M. Y., 1986 *Phys. Rev. Lett.* **57**, 2037

White, W. II., 1982 *J. Colloid Interface Sci.* **87**, 204

Wiesmann, H. J. and Pietronero, L., 1986 in *Fractals in Physics* edited by L. Pietronero and E. Tossati (North-Holland, Amsterdam) p. 151

Wilkinson, D. and Willemsen, J., 1983 *J. Phys.* **A16**, 3365

Willemsen, J., 1984 *Phys. Rev. Lett.* **52** 2197

Witten, T. A. and Sander, L. M., 1981 *Phys. Rev. Lett.* **47**, 1400

Witten, T. A. and Sander, L. M., 1983 *Phys. Rev.* **B27**, 5686

Witten, T. A., 1985 in *Physics of Finely Divided Matter* edited by N. Boccara and M. Daoud (Springer, New York) p. 212

Wolf, D. E., 1987 *J. Phys.* **A20**, 1251

Wolf, D. E. and Kertész, J., 1987a *J. Phys.* **A20**, L257
Wolf, D. E. and Kertész, J., 1987b *Europhys. Lett.* **4**, 561
Zabolitzky, J. G. and Stauffer, D., 1986 *Phys. Rev.* **A34**, 1523
Ziff, R. M., Cummings, P. T. and Stell, G., 1984 *J. Phys.* **A17**, 3009
Ziff, R. M. and McGrady, E. D., 1985 *J. Phys.* **A18**, 3027
Ziff, R. M., McGrady, E. D. and Meakin, P., 1985 *J. Chem. Phys.* **82**, 5269
Ziff, R. M., 1986 *Phys. Rev. Lett.* **56**, 545